

R-04-57

Single-well injection-withdrawal tests (SWIW)

Investigation of evaluation aspects under heterogeneous crystalline bedrock conditions

Rune Nordqvist, Erik Gustafsson
Geosigma AB

August 2004

Svensk Kärnbränslehantering AB

Swedish Nuclear Fuel
and Waste Management Co

Box 5864

SE-102 40 Stockholm Sweden

Tel 08-459 84 00

+46 8 459 84 00

Fax 08-661 57 19

+46 8 661 57 19



Single-well injection-withdrawal tests (SWIW)

Investigation of evaluation aspects under heterogeneous crystalline bedrock conditions

Rune Nordqvist, Erik Gustafsson
Geosigma AB

August 2004

This report concerns a study which was conducted for SKB. The conclusions and viewpoints presented in the report are those of the authors and do not necessarily coincide with those of the client.

A pdf version of this document can be downloaded from www.skb.se

Abstract

Single-well injection-withdrawal (SWIW) tracer tests have been identified by SKB as an investigation method for solute transport properties in the forthcoming site investigations. A previous report /Nordqvist and Gustafsson, 2002/ presents a literature study as well as scoping calculations for SWIW tests in homogeneous crystalline bedrock environments. The present report comprises further scoping calculations under assumptions of heterogeneous bedrock conditions. Simple but plausible homogeneous evaluation models are tested on simulated SWIW tests in hypothetical heterogeneous two-dimensional fractures. The results from this study indicate that heterogeneity may cause effects of flow irreversibility when background hydraulic gradients are significant and the tested section is located in a dominating flow path. This implies that such conditions make it more difficult to interpret results from SWIW tests of longer duration with sorbing and/or diffusing tracers. Sorption and diffusion processes may be best studied when SWIW tests are conducted in borehole sections with low natural flow rates.

Contents

| | | |
|----------|---|----|
| 1 | Introduction | 7 |
| 2 | Objectives | 9 |
| 3 | Approach | 11 |
| 3.1 | General outline | 11 |
| 3.2 | Simulation of heterogeneous fractures | 11 |
| 3.3 | Collection of independent information | 11 |
| 3.4 | Simulation of SWIW tests | 12 |
| 3.5 | Evaluation of simulated SWIW tests | 14 |
| 3.5.1 | General | 14 |
| 3.5.2 | Parameter estimation method | 15 |
| 3.5.3 | Estimation scenarios | 17 |
| 4 | Results | 19 |
| 4.1 | Overview of simulated cases | 19 |
| 4.2 | Base case simulations | 20 |
| 4.2.1 | Evaluation of the base case simulation results | 24 |
| 4.3 | Simulations with a hydraulic gradient | 26 |
| 4.3.1 | Evaluation of the base case with hydraulic gradient | 30 |
| 4.3.2 | Tracer injection in a major flow path | 33 |
| 4.4 | Case 2 simulations | 36 |
| 4.5 | Simulations with sorbing tracers | 38 |
| 4.5.1 | Base case simulations | 38 |
| 4.5.2 | Sorbing tracers with a hydraulic gradient | 40 |
| 4.5.3 | Implications for interpretation of matrix diffusion effects | 42 |
| 5 | Summary and conclusions | 45 |
| 6 | References | 47 |

1 Introduction

Single-well injection-withdrawal (SWIW) tracer tests have been identified by SKB as an investigation method for solute transport properties in the forthcoming site investigations. A previous report /Nordqvist and Gustafsson, 2002/ presents a literature study as well as scoping calculations for SWIW tests in expected crystalline bedrock environments. The scoping calculations focussed on simulation of flow and transport processes, identification of experimental constraints and tracer analysis demands. The study covered a number of aspects related to experimental issues such as feasible bedrock conditions (depths, transmissivities, etc), experimental pumping rates during tracer injection and withdrawal, duration of various experimental phases, etc.

One part of the above study discusses test interpretation issues and identified conditions for identification of transport processes and estimation of transport model parameters. This analysis was carried out by studying parameter sensitivities and correlation between parameters for various assumed estimation scenarios. Thereby it was possible, for a few basic scenarios, to identify which parameters that may be possible to identify/estimate simultaneously from a SWIW test.

The previous scoping calculations were very basic in their nature and therefore based on assumptions of homogenous bedrock conditions. The results of the study suggest that SWIW tests are applicable in crystalline rock for expected ranges of hydraulic properties of the rock. As a complement and extension of the previous study, a need for further scoping calculations were identified for a more in-depth study of test interpretation aspects under heterogeneous bedrock conditions.

This report describes an extended theoretical study of SWIW tests under heterogeneous conditions. The purpose of the project is to study the importance of heterogeneity on interpretation of test results. In the present study the ability of simple, but plausible, evaluation models (i.e. homogenous models) to obtain flow and transport properties in heterogeneous systems is tested. In actual field tests, it is likely that information about heterogeneity will be limited and that a “standard” evaluation tool will be based on assumptions of homogeneity. One intention in this study is to gain further insight into interpretation difficulties, from SWIW test results, that may arise due to heterogeneity.

Related studies, which provide valuable background information for this type of test, have been presented by /Tsang, 1995/, /Altman et al, 2000/ as well as /Lesshoff and Konikow, 1997/. The results from these and other studies have also been summarised by /Nordqvist and Gustafsson, 2002/.

2 Objectives

The objectives for the present study may be summarised as follows:

- Describe and demonstrate an inverse modelling evaluation tool for SWIW tests based on homogeneous assumptions
- Perform inverse modelling (i.e. parameter estimation) on simulated tests in heterogeneous systems in order to investigate the applicability of typical basic evaluation approaches on experimental results obtained in heterogeneous environments.

3 Approach

3.1 General outline

The basic approach is to simulate heterogeneous fractures and then to simulate SWIW tests in the fractures. The resulting tracer recovery breakthrough curves are regarded as “field” measurements to be interpreted with typical simplified evaluation approaches.

In addition, supporting measurements are considered. These include estimates of transmissivity and through-flow in the tested section. It is generally assumed that such information will be available prior to the performance of SWIW tests. In this study, these values will usually be regarded as “known”. Alternatively, they may be obtained by actually simulating and evaluating fluid injection tests and dilution tests as would be done in actual field applications. The latter is done, for demonstration purposes, to a limited extent in this study.

The general approach may be described by the following steps:

1. Simulation of heterogeneous fractures.
2. Collection of independent information.
3. Simulation of SWIW tests in simulated heterogeneous fractures.
4. Evaluation of SWIW tests.

Each of the steps is described in more detail below.

3.2 Simulation of heterogeneous fractures

Synthetic heterogeneous fractures are created by a commonly used method called the turning bands method /Mantoglou and Wilson, 1989/. Spatially correlated transmissivity fields represent the heterogeneity. Commonly used ranges for the spatial statistics (mean, variance and correlation length) are selected to create fractures with different degrees of heterogeneity.

3.3 Collection of independent information

Independent information primarily includes values of transmissivity and (natural) flow through the test section. As shown by the previous scoping calculations /Nordqvist and Gustafsson, 2002/, this information must be available prior to performing SWIW-tests in order to find a suitable experimental design. In this study, values for these attributes are either assumed known or estimated by simulated tests. If assumed known, values are simply obtained from parameter settings of the current simulation model. If considered unknown, values are obtained by simulating and evaluating, using “standard” methods, hydraulic injection tests and dilution tests, respectively. In general, the alternative with “known” values are used, while the alternative with a complete evaluation sequence are used for demonstration purposes only.

3.4 Simulation of SWIW tests

The SWIW tests are simulated using a similar experimental sequence as in the previous scoping calculations, including the following phases:

1. Injection of one or more tracers with a constant fluid flow rate.
2. Injection of chaser fluid at a constant flow rate. During this phase, the tracer is pushed out further into the tested rock volume.
3. Waiting phase with no flow. This phase may primarily be employed when natural gradients are low and when the specific purpose is to study time-dependent transport processes.
4. Recovery phase. During this phase, water is pumped back to the tested section and the resulting tracer breakthrough curve is collected.

A schematic example of a resulting breakthrough curve during a SWIW test is shown in Figure 3-1.

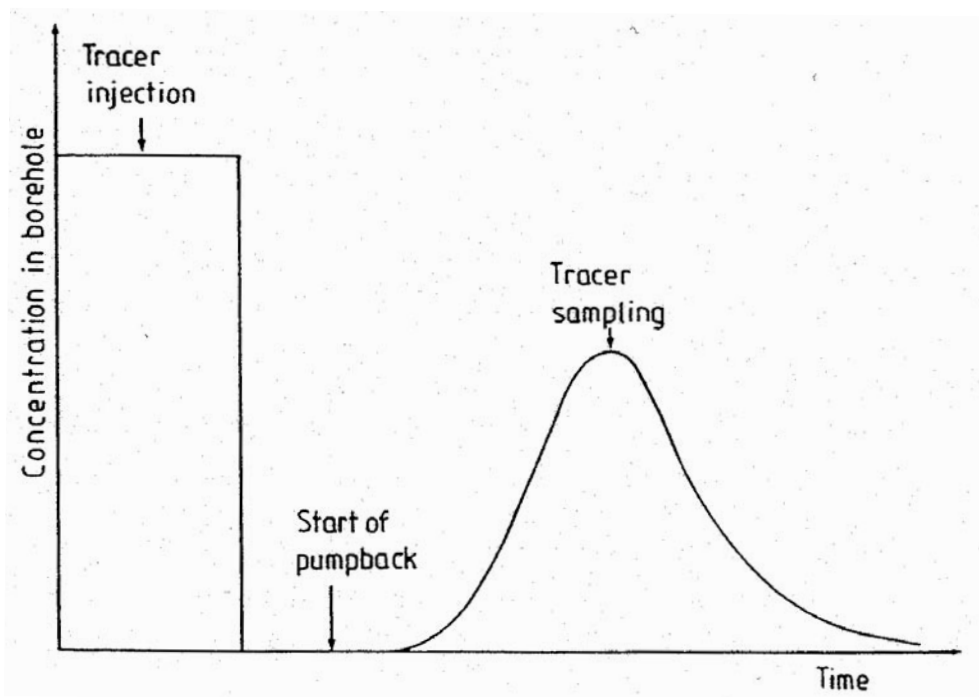


Figure 3-1. Schematic tracer concentration sequence during a SWIW test /from Andersson, 1995/.

The specific design (flow rates, durations, etc) of each simulated test will depend on factors such as transmissivity (estimated from hydraulic tests) and hydraulic background gradient (derived from dilution measurements).

The simulations are carried out numerically using the finite element code SUTRA /Voss, 1984/. Simulations of the entire test sequence entails a series of coupled SUTRA simulations, where simulation results from one phase is used as initial conditions to the following phase. All simulations are carried out assuming steady-state flow conditions and transient transport conditions. The governing flow equation may be given as:

$$\frac{\partial}{\partial x} \left(T \frac{\partial h}{\partial x} \right) + \frac{\partial}{\partial y} \left(T \frac{\partial h}{\partial y} \right) + Q = 0 \quad (3-1)$$

where T is the transmissivity (L^2/T), h the hydraulic head (L), and Q represent fluid point sources (L^3/T). The magnitude of the average fluid velocity, v (L/T), is calculated from the head solution by:

$$v = -\frac{K}{p} \nabla h \quad (3-2)$$

where K is the hydraulic conductivity (L/T) and p the flow porosity (dimensionless). The computed velocities are used as input for an advection-dispersion transport equation which may be described by:

$$D_L \frac{\partial^2 C}{\partial S_L^2} + D_T \frac{\partial^2 C}{\partial S_T^2} - \frac{\partial(v_L C)}{\partial S_L} = R \frac{\partial C}{\partial t} \quad (3-3)$$

where S_L and S_T are coordinates (L) directed along and perpendicular, respectively, to the direction of flow, D_L and D_T are the longitudinal and transverse dispersion coefficients (L^2/T), R is the retardation factor (dimensionless) due to linear equilibrium sorption, and C is the concentration (M/L^3). The dispersion coefficients are assumed to be proportional to the magnitude of the velocity:

$$D_L = a_L v_L \quad (3-4)$$

$$D_T = a_T v_L \quad (3-5)$$

where a_L and a_T are values of the longitudinal and transverse dispersivities (L), respectively.

Although transient flow effects would be present in the head distribution around the tested borehole sections, previous scoping calculations indicated that effects on tracer breakthrough curves are relatively small. For scoping calculations such as these, involving numerous simulations, neglecting transient effects on heads decreases simulation times considerably. However, for future actual field applications it may be appropriate to re-evaluate whether transient flow effects should be considered in test planning and evaluation.

The simulation set-up consists of a 50 m x 50 m domain with the tested borehole in the centre. The extent of the domain is considerably larger than the expected rock volume that the injected tracer occupies at the end of the chaser fluid phase. The boundary conditions are constant head around the entire perimeter of the model domain, which may be readily used to create a natural hydraulic background (i.e. natural groundwater flow) through the system. The tested borehole section in the centre is simulated as a well with a constant flow rate. During the tracer injection phase, in-flowing water is assigned a constant concentration.

The finite element mesh consists of 62,500 equally sized elements with dimensions of 0.2 x 0.2 m.

The main results extracted from the simulations are tracer breakthrough curves from the recovery phase, when water is pumped back to the borehole.

The applied simulation model is based on an equivalent porous media approach. The specific values chosen for various parameters such as transmissivity, hydraulic conductivity, flow porosity, etc, comprise some type of effective values for various properties and are valid only for this particular conceptualisation. For example, transmissivity and porosity should in this model be interpreted to be representative for the test section interval (generally assumed to be 1 meter in the simulations). Transmissivity is a measure of the total capacity of the section to conduct water flow, while the porosity gives a measure of the volume available for the flowing water. In other model conceptualisations, these and other parameters may be named and defined differently but the main mechanisms for flow and transport are likely to be similar. Thus, the results from the scoping calculations in this report should have a large degree of generality. The choice of simulation code in this study is based on computational flexibility, numerical reliability and that it is a well-established code that continuously is updated and subject to extensive quality control.

3.5 Evaluation of simulated SWIW tests

3.5.1 General

The interpretation of simulated SWIW tests is made in an inverse modelling mode, where model parameter values are determined from experimental results. Commonly, this is also referred to as calibration or parameter estimation. In this report, the term parameter estimation will be preferred most of the time because it provides the closest description of what is actually done. Estimation of parameter values is in this study carried out using non-linear regression, where estimation statistics are obtained simultaneously. The flow and transport model used in estimation is what may be considered a typical simple evaluation tool, i.e. a homogenous model. Other evaluation approaches are also possible. However, it is conceivable that only limited information about heterogeneity will be available and that a homogeneous evaluation approach will at least be part of a “standard” evaluation of a SWIW test.

The simulation model used for the parameter estimation is identical to the one described in section 3.4, except that homogeneous conditions with respect to T (transmissivity) is assumed. Typical estimation parameters (see section 3.4) considered here include p (porosity), a_L (longitudinal dispersivity), initial concentration and R (retardation factor).

3.5.2 Parameter estimation method

Parameter estimation is a central part of this study and therefore a relatively detailed discussion of such aspects is presented in the rest of this section.

Estimated parameter values are obtained by non-linear least-squares regression. The basic non-linear least-squares regression minimises the sum of squared differences between the modelled (Y^M) and the observed (Y^O) variables and may be formulated as:

$$\text{Min } S = \mathbf{E}_R^T \mathbf{W} \mathbf{E}_R \quad (3-6)$$

where \mathbf{E}_R is a vector of residuals ($Y^M - Y^O$) and \mathbf{W} is a vector of reliability weights on observations.

The specific method for carrying out the regression employed in this study is often referred to as the Marquardt-Levenberg method /Marquardt, 1963; Levenberg, 1944/. This method is a Newton-type optimisation algorithm that finds the parameter values that minimises the sum of squared errors between model and measurement values in an iterative manner. A simplified version of the search algorithm used may be written as:

$$\mathbf{B}_{r+1} = \mathbf{B}_r + (\mathbf{X}_r^T \mathbf{W} \mathbf{X}_r)^{-1} \mathbf{X}_r^T (\mathbf{Y}^O - \mathbf{Y}_r^M) \quad (3-7)$$

where \mathbf{B} is a vector of parameter estimates, \mathbf{X} is a parameter sensitivity matrix, and the subscripts r and $r+1$ refer to the iteration number.

Given an initial parameter estimate, eq (3-7) is repeated until a local optimal solution is found. The local minimum is defined by some convergence criterion, for example when parameter estimates are essentially identical between iterations. Finding a local minimum does not guarantee that the global minimum is found. When this appears to be a problem, several sets of initial estimates may be tried. When some knowledge about the parameters to be estimated and the physical system is already available, the initial estimates are often good enough for ensuring that a global minimum is found.

An important element of the above procedure is the matrix containing the parameter sensitivities. Parameter sensitivity is defined as the partial derivative of the dependent (simulated) variable with respect to a parameter. A sensitivity matrix contains one row for each observation and one column for each estimated parameter, as in the following example with three observations and two parameters.

$$\mathbf{X} = \begin{pmatrix} \frac{\partial y_1}{\partial b_1} & \frac{\partial y_1}{\partial b_2} \\ \frac{\partial y_2}{\partial b_1} & \frac{\partial y_2}{\partial b_2} \\ \frac{\partial y_3}{\partial b_1} & \frac{\partial y_3}{\partial b_2} \end{pmatrix} \quad (3-8)$$

The computation of sensitivities is, in this study, accomplished by using a relatively simple forward central difference scheme. This means that the simulation model must be run $1 + P$ times (P being the number of parameters) for each iteration.

Parameter sensitivities may be used to determine the precision of the estimated parameter values. Given below are two diagnostic measures regarding parameter uncertainty that may be obtained as a result of regression /Cooley, 1979/.

The *standard errors* of parameter estimates are obtained by taking the square roots of the diagonals in the parameter covariance matrix, which is given by:

$$s^2(\mathbf{X}^T\mathbf{W}\mathbf{X})^{-1} \quad (3-9)$$

with s^2 being the error variance:

$$s^2 = \frac{\sum_{i=1}^N w_i (y_i^O - y_i^M)^2}{N - P} \quad (3-10)$$

where N is the number of measurements, P the number of parameters and w_i the weight on observation i .

The linear correlation $r(p_1, p_2)$ between two parameters p_1 and p_2 is expressed by:

$$r(p_1, p_2) = \frac{\text{Cov}(p_1, p_2)}{\sqrt{\text{Var}(p_1) \text{Var}(p_2)}} \quad (3-11)$$

where the variance and covariance terms are elements of the $s^2(\mathbf{X}^T\mathbf{W}\mathbf{X})^{-1}$ matrix. The correlation is a measure of the inter-dependence between two parameter estimates and correlation values range between -1 and 1 . Values close to either -1 or 1 mean that a change in one parameter value may be compensated for by a similar change in another parameter value to maintain the same fit (sum of squares) between model and measurements.

The standard errors and parameter correlation values are the main diagnostic measures used in this study when examining the parameter estimation results from evaluation of the simulated SWIW tests.

The inter-dependence between parameters, as given by the parameter correlation values, is a major reason why estimation of some parameter combinations fails. This feature is, thus, also a valuable design tool which was used in the preceding study /Nordqvist and Gustafsson, 2002/ to study parameter identification aspects.

One way to reduce excessive correlation is to combine more than one type of observation data in regression or to combine data obtained under different field conditions. In regression with multiple-type observation data, the weights, \mathbf{W} , also function as a scaling method to account for the different magnitudes in observation data types.

The use of concentration measurements from different solutes simultaneously in regression, especially when these have different transport properties may be considered a case of multiple-type observation data. For illustration purposes a simple one-dimensional example is given of a case when it is actually necessary to have at least two such data sets. This example is when the retardation coefficient R , is determined using a standard one-dimensional solute transport model with advection and dispersion (see for example /Van Genuchten and Alves, 1982/):

$$R \frac{\partial C}{\partial t} = D_1 \frac{\partial^2 C}{\partial l^2} - v \frac{\partial C}{\partial l} \quad (3-12)$$

where l is the coordinate in the direction of the transport path [L], t is time [T], D_1 is the longitudinal dispersion coefficient [L^2/T], and v is the average water velocity [L/T]. In order to estimate R , v , and D_1 one needs to have two data sets, one with a retarded and

one with a non-retarded solute. When breakthrough curves from tracer tests are obtained, a common procedure is to estimate v and D_1 from each curve individually (the retarded curve would give “apparent” values of these parameters) and then obtain R as the ratio of the two velocities.

Instead of the procedure described above, one may use both data sets simultaneously in regression. It is very straightforward to construct the sensitivity matrix for this case, assuming there are m observations with the non-retarded tracer and n observations with the retarded tracer:

$$\mathbf{X} = \begin{pmatrix} \frac{\partial C_1}{\partial v} & \frac{\partial C_1}{\partial D_1} & 0 \\ \frac{\partial \dot{C}_m}{\partial v} & \frac{\partial \dot{C}_m}{\partial D_1} & \cdot \\ \frac{\partial C_{m+1}}{\partial v} & \frac{\partial C_{m+1}}{\partial D_1} & \frac{\partial C_{m+1}}{\partial R} \\ \frac{\partial \dot{C}_{m+n}}{\partial v} & \frac{\partial \dot{C}_{m+n}}{\partial D_1} & \frac{\partial \dot{C}_{m+n}}{\partial R} \end{pmatrix} \quad (3-13)$$

In addition to making it possible to estimate R directly, this would also be expected to decrease estimation errors for the other parameters (v and D_1) simply because more observations are included in the regression. This example illustrates that the use of multiple-type data in regression is not very different than using single-type data. It is mostly a matter of arranging the sensitivity matrix and applying proper observation weights. An example of this type of evaluation in one-dimensional transport, and that also includes matrix diffusion in addition to surface sorption, is presented in /Andersson et al, 2003/.

In this study, the method described above is used for estimation of sorption parameters. A two-dimensional transport model is used instead of the one-dimensional in the example above, but the general evaluation principle of using multiple data sets simultaneously is the same. This approach was also used from an experimental design perspective in the preceding study /Nordqvist and Gustafsson, 2002/, and a similar design analysis was also presented by /Nordqvist, 1998/.

3.5.3 Estimation scenarios

The various estimation scenarios studied in this report may be sorted into the following main categories of experimental conditions:

- Estimation of parameters without hydraulic gradient.
- Estimation of parameters when background gradient is significant.
- Estimation of equilibrium sorption parameters (i.e. retardation coefficients), assuming that more than one tracer with different sorption properties are injected simultaneously.

It has been demonstrated in the previous scoping calculations /Nordqvist and Gustafsson, 2002/ that, unlike cross-hole tracer tests, parameters such as advective porosity and dispersivity may not be estimated simultaneously unless there is a hydraulic background gradient present. In such cases one may assume that advective porosity (i.e. fracture width) is known independently from other borehole measurements. Alternatively, another approach may be to make several assumptions about the value of dispersivity and then estimate the advective porosity (or equivalent) for each assumed value, thereby obtaining a plausible interval for the porosity.

4 Results

4.1 Overview of simulated cases

Simulated SWIW tests are created and interpreted for two selected main scenarios of different heterogeneity characteristics. The selection of the studied cases is made so that one case (Case 1) has a small degree of heterogeneity and Case 2 has a larger degree of heterogeneity. For both cases, several variants are studied with different well placements, estimation parameters, hydraulic gradients and sorption.

It may be pointed out that this study is limited with respect to possible variants of heterogeneity characteristics or possible alternative approaches to describe heterogeneity. There are many combinations of variance, correlation length and spatial correlation models that may be considered. Further, for each such assumption, many realisations may be studied.

Base case – Case 1

This case was constructed to be as simple as possible assuming relatively moderate transmissivity heterogeneity.

The following experimental settings and values of hydrogeologic parameters were used:

- Tracer injection phase duration = 3 600 seconds = 60 minutes = 1 h.
- Chaser fluid injection phase duration = 36 000 s = 600 min = 10 h.
- Flow during injection, chaser and extraction phases = $1.0 \times 10^{-6} \text{ m}^3/\text{s}$.
- Concentration of tracer in in-flowing water = 1.0 mass units/ m^3 .
- Porosity = 0.001.
- Longitudinal dispersivity = 0.1 m.
- Transverse dispersivity = 0.01 m.

The heterogeneous transmissivity field was generated as with the following features:

- Average $T = 1.0 \times 10^{-6} \text{ m}^2/\text{s}$.
- Variance ($\ln T$) = 1.0.
- Correlation length = 2.0 m (exponential variogram model).

Case 2

- Average $T = 1.0 \times 10^{-6} \text{ m}^2/\text{s}$.
- Variance ($\ln T$) = 5.0.
- Correlation length = 5.0 m.
- Other parameters and experimental settings as above.

4.2 Base case simulations

The generated heterogeneous transmissivity ($\ln T$) field for the base case is shown in Figure 4-1. The image of the distribution is approximate, as it shows colour zones of contoured values of the $\ln(T)$ distribution. The well is placed, somewhat arbitrary, slightly to the left of the centre of the simulated fracture because in a subsequent section a hydraulic background gradient is added, making the background flow direction parallel with the x-axis towards the right-hand side of the fracture in Figure 4-1.

Contours of calculated heads during the injection and chaser fluid phases are shown in Figure 4-2. An illustration of the heterogeneous flow pattern during the tracer injection and chaser fluid phases is shown in Figure 4-3, where flow vectors are plotted.

The tracer plume at the end of the tracer injection period (one hour) is shown in Figure 4-4 and the corresponding plume at the end of the chaser fluid phase (10 hours) is shown in Figure 4-5. The simulated tracer concentration in the tested well for the base case is illustrated in Figure 4-6.

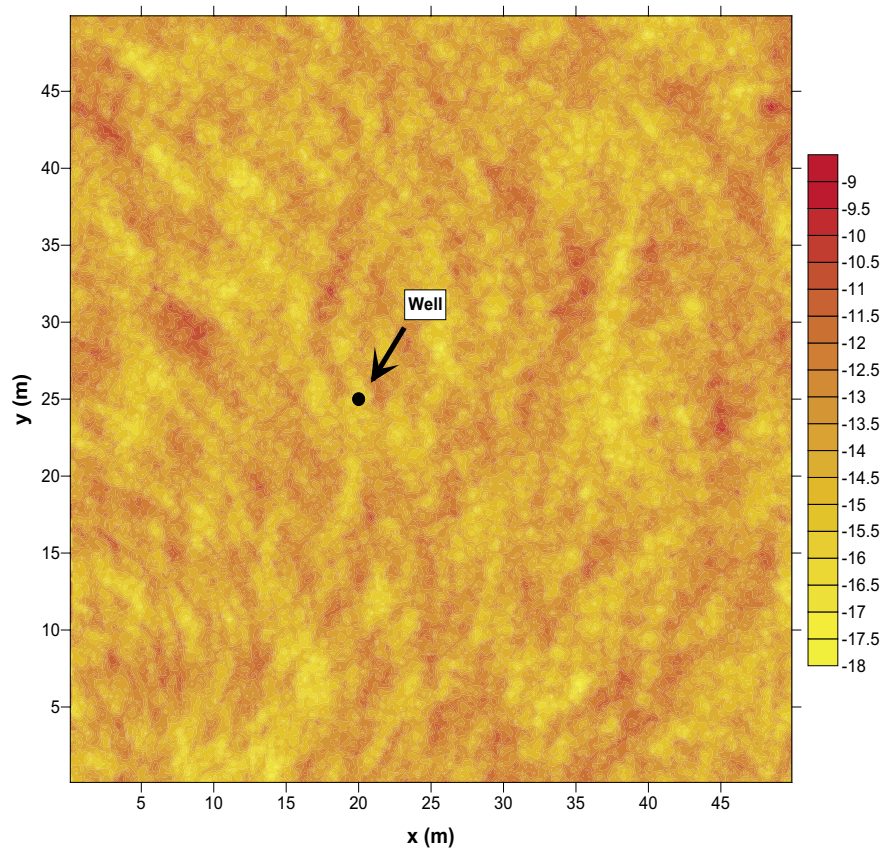


Figure 4-1. Spatial distribution of $\ln T$ for the base case simulation.

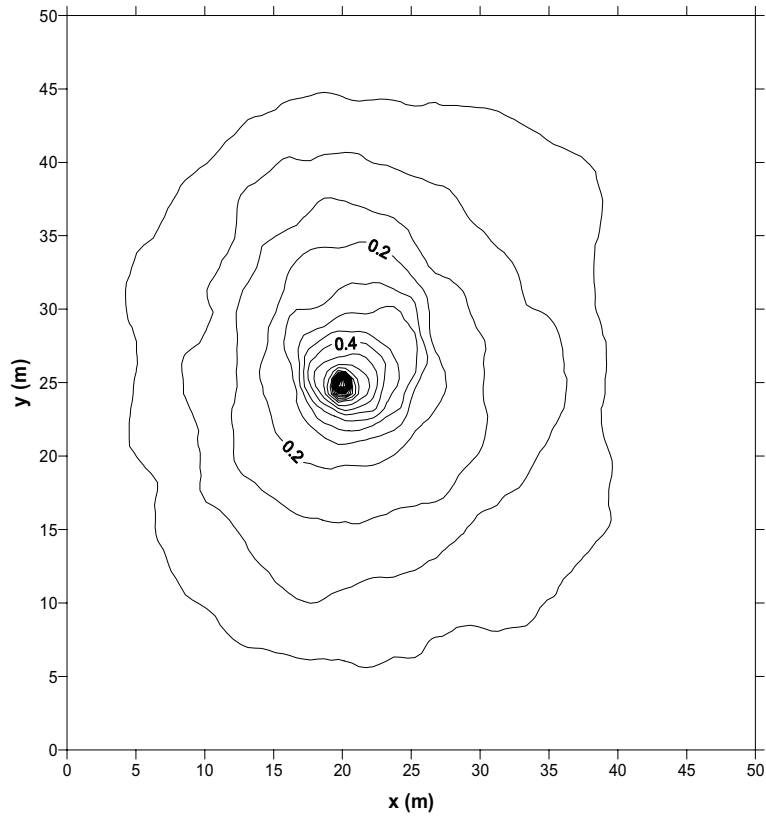


Figure 4-2. Hydraulic head distribution during the injection and chaser fluid phases. The simulated head in the well is about 6.25 m.

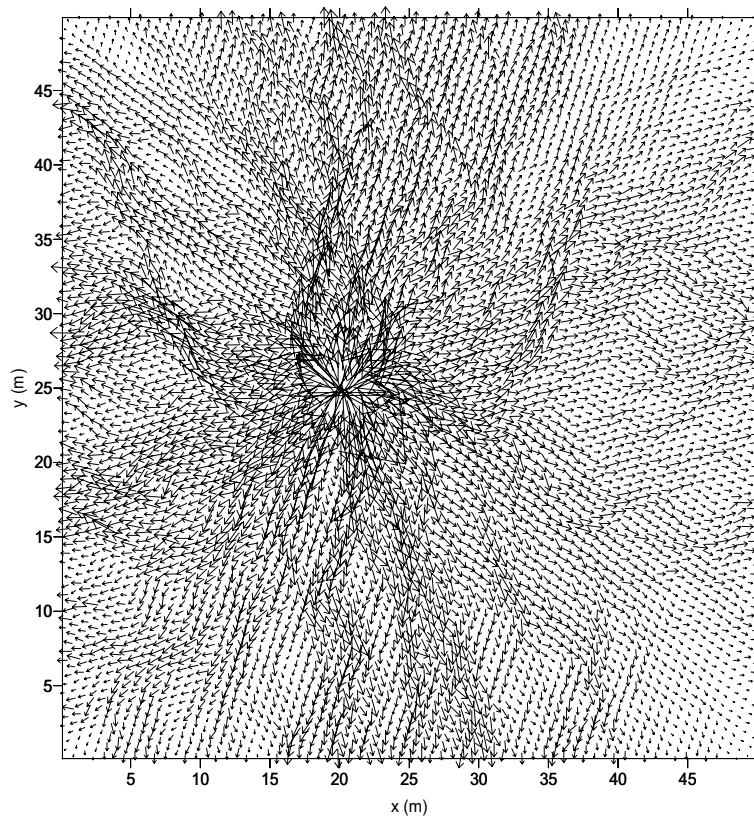


Figure 4-3. Flow vectors during the injection and chaser fluid phases. The lengths of the vectors indicate relative magnitudes of the fluid velocity.

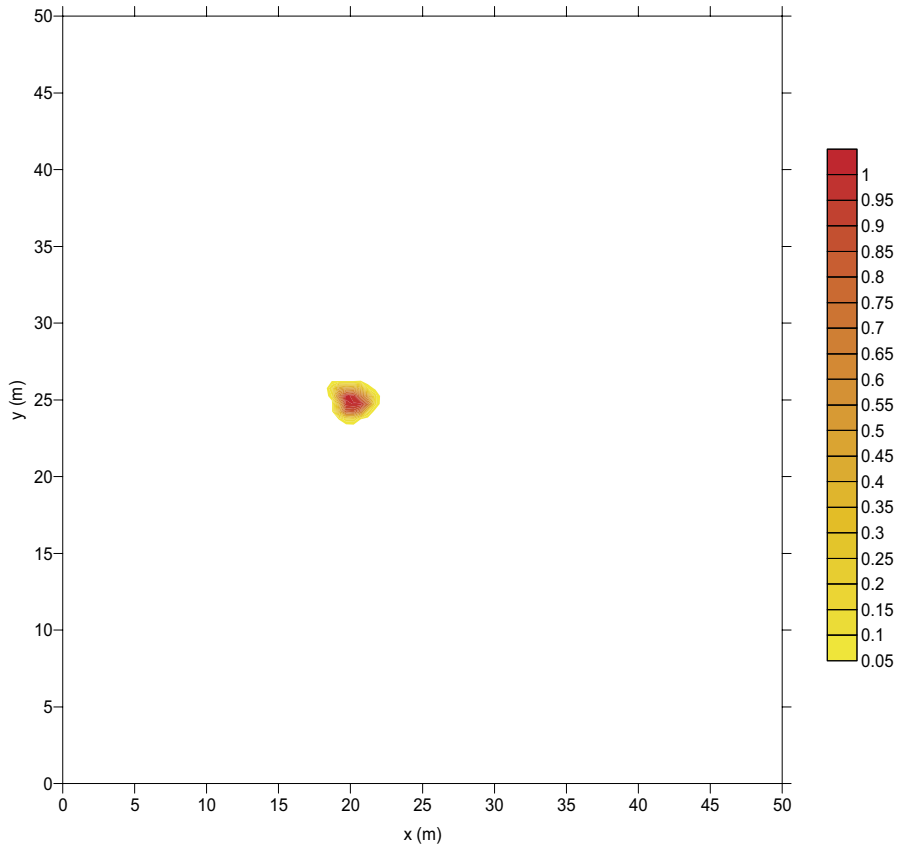


Figure 4-4. Tracer concentration distribution at the end of the injection phase (60 minutes).

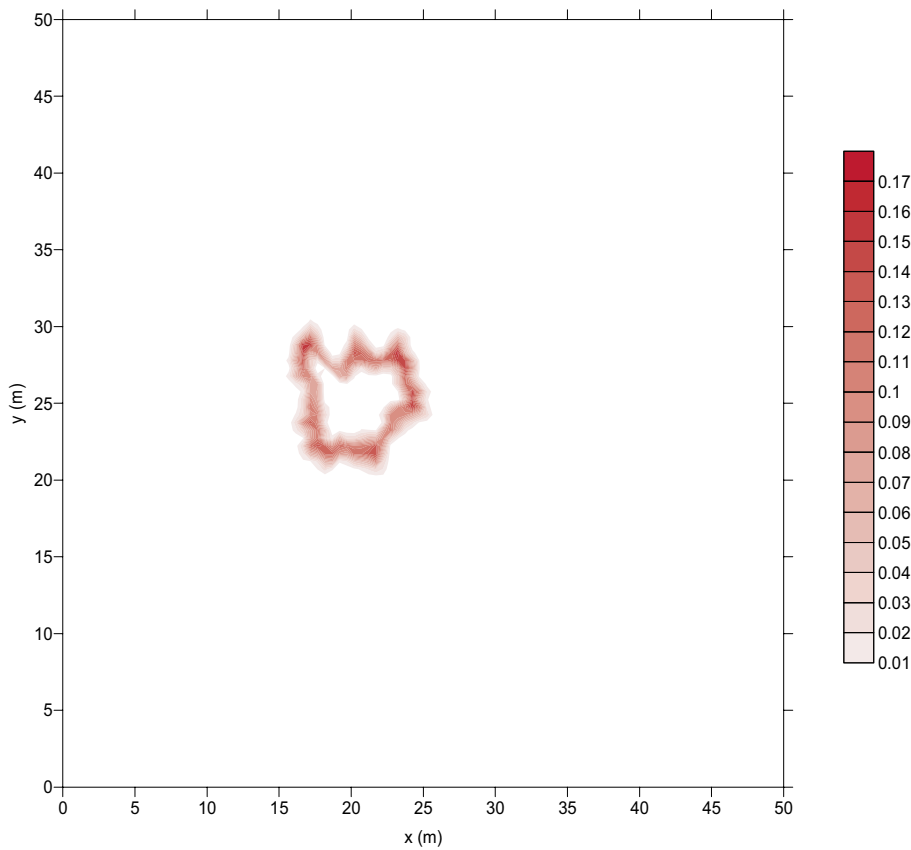


Figure 4-5. Tracer concentration distribution at the end of the chaser fluid phase (10 hours).

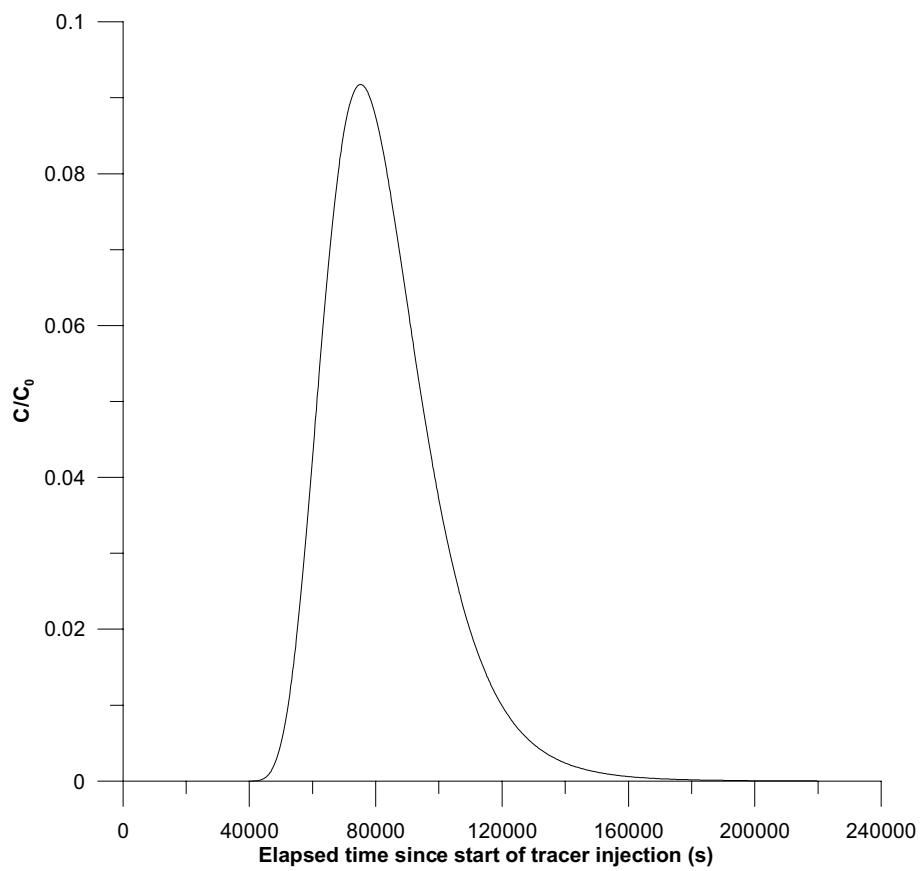
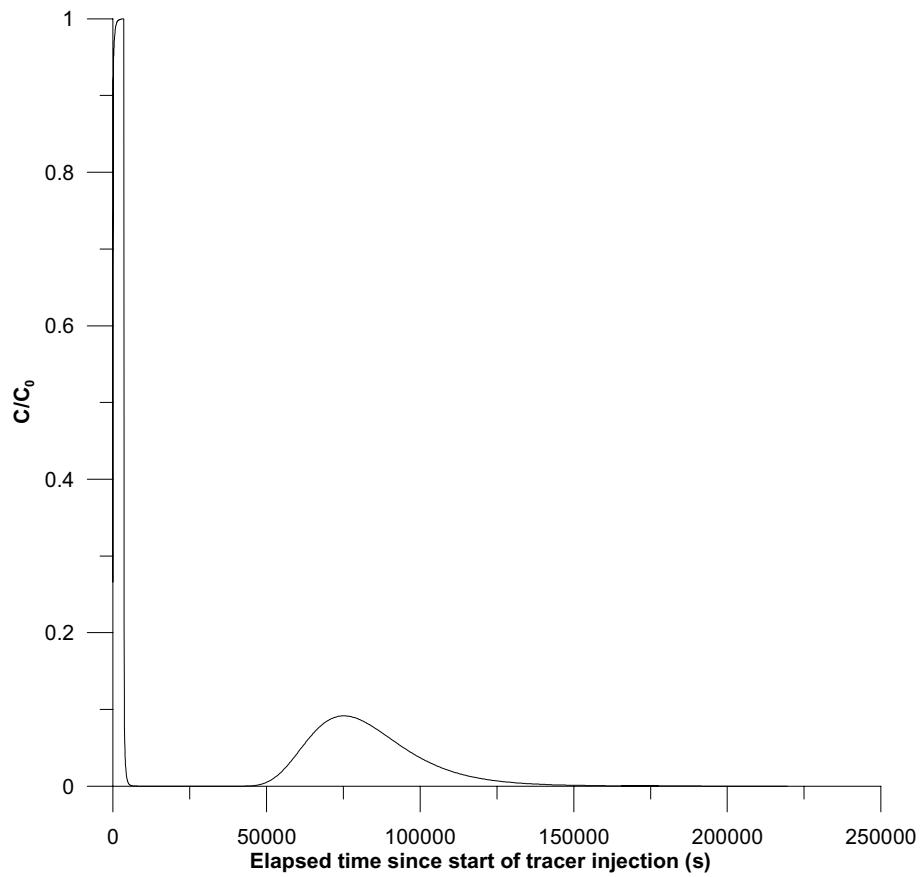


Figure 4-6. Tracer concentration in the tested borehole section during the entire experimental sequence (top) and tracer breakthrough curve during the tracer recovery phase (bottom).

4.2.1 Evaluation of the base case simulation results

The basic tool for evaluation of the base case, as well as all other cases below, is based on a homogenous two-dimensional model of similar size as the experimental simulation model. The homogenous simulation model is used to provide values of Y^M (simulated dependent variables) and of X (the sensitivity matrix) to the parameter estimation algorithm described in section 3.5.

The parameter estimation runs require input of experimental design attributes such as duration of different phases, flows, injection concentration, etc, as well as initial guesses for estimated parameters.

In all parameter estimation calculations one must make choices about which parameters are to be estimated and which should be considered known. In cross-hole tracer tests, when no processes such as sorption and diffusion occur, often a one-dimensional advection-dispersion model is used and typical estimation parameters might be residence time, dispersivity and possibly also the injection concentration or equivalent (see for example /Andersson et al, 2002/).

Similar parameters may also be considered in the present case, although in the two-dimensional model used here the residence time is replaced by the porosity. In the previous SWIW-study /Nordqvist and Gustafsson, 2002/ it was, through a sensitivity analysis, demonstrated that it should not be possible to reliably estimate the porosity and the dispersivity simultaneously in the absence of a natural hydraulic gradient because of the linear dependence between these parameters. This is a disadvantage of SWIW tests compared with cross-hole tracer tests.

A regression analysis was made on the base case breakthrough curve with porosity (p), the longitudinal dispersivity (a_L) and a factor (pf) proportional to the tracer injection concentration. Despite the known linear dependence between the porosity and the longitudinal dispersivity, the regression algorithm converged relatively satisfactorily. The best-fit results for this case are shown in Figure 4-7 below.

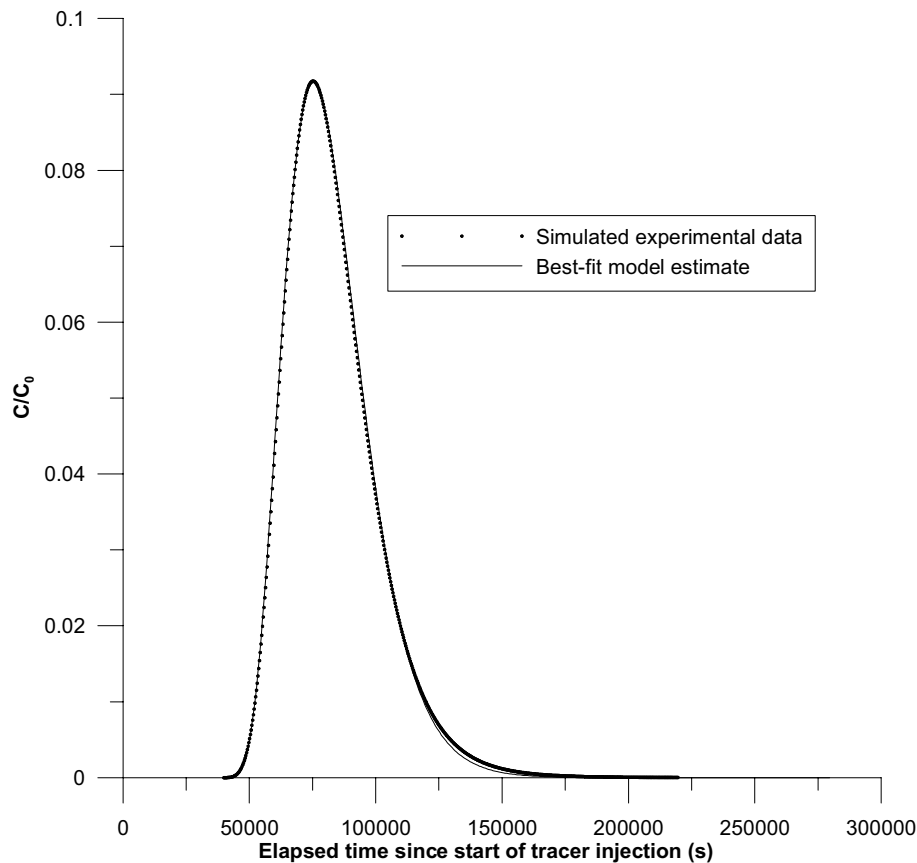


Figure 4-7. Regression results for estimation of p , a_L and pf using the simulated base case experimental results.

The final parameter estimates were as follows (with standard errors in percent of the estimated value):

$$p = 6.26 \times 10^{-4} \text{ (13.6)}$$

$$a_L = 0.125 \text{ m (6.27)}$$

$$pf = 0.995 \text{ (0.08)}$$

The linear correlations between the estimated parameters were as follows:

$$p - a_L \quad -0.9996$$

$$p - pf \quad -0.3798$$

$$a_L - pf \quad 0.3953$$

The high correlation between the porosity and longitudinal dispersivity were very close to one, as expected. The fact that the regression analysis, despite the high correlation, converges to a result with relatively low standard errors is due to the extremely close fit between model and experimental data which results in a very low value of s^2 in eq 3-5. However, in a real field experiment the experimental noise would likely be considerably larger and the standard errors also considerably larger. In any case, one should be very critical of any parameter estimation results that provide such large correlation values between parameters.

A comparison with a simpler estimation scenario, where only a_L and pf are estimated and p assumed known (set to the “true” value of 1×10^{-3}), gives the following result:

$$a_L = 0.09726 \text{ m (0.214)}$$

$$pf = 0.9899 \text{ (0.077)}$$

The correlation between a_L and pf was in this case 0.593. The resulting standard errors indicate that this parameter set is much more reliably estimated than in the preceding case.

Because of the high correlation between p and a_L it is obvious that the estimated value of one parameter is sensitive to the value of the other. Thus, in the latter case a different dispersivity value would be obtained if a different porosity value would be used, which also is indicated from the results of the two cases above. In an alternative regression run where the porosity was assumed to be 2×10^{-4} , the resulting value of a_L was 0.213 m.

In a real field test, the porosity (or corresponding parameter) will likely not be well known prior to a SWIW test other than estimates made from core logging, etc.

4.3 Simulations with a hydraulic gradient

As a variation of the base case, a natural hydraulic background gradient was added to the system. This was accomplished by modifying the constant head values along the perimeter of the model so that an average uniform gradient of 0.02 was obtained. Such a model set-up will create dominating flow paths that are initialised at parts of the inflow boundaries where the transmissivity values are largest. This makes the resulting flow field somewhat of an artefact of the boundary conditions, but such effects are not important for the present analysis of SWIW tests.

The simulated flow field without any pumping in the tested well is shown, using flow vectors, in Figure 4-8. The relatively moderate heterogeneity creates a pattern of a few flow “channels” with higher flows. The well location is the same as in the base case above and it may be observed that the well happens to be located in a patch of relatively low flow rates.

The corresponding flow pattern during the fluid injection phases (tracer injection and chaser fluid) is shown in Figure 4-9. The fluid injection changes the flow pattern considerably compared with the case without pumping (Figure 4-8), but is also somewhat different than the corresponding flow field without a natural background gradient in Figure 4-3.

The steady-state hydraulic head field during the fluid injection phases is shown in Figure 4-10 and the tracer plume at the end of the chaser phase in Figure 4-11.

The resulting tracer recovery breakthrough curve from a simulated SWIW test (with experimental settings identical to the base case) is shown in Figure 4-12, where the corresponding breakthrough curve for the base case also is shown. The differences between the two curves are expected. A slightly earlier first arrival and a more elongated tail occur for the gradient case because a downstream drift component acts on the tracer throughout the simulated experiment. The difference would become more pronounced the longer the experimental phases are (and even more so with the addition of a waiting phase).

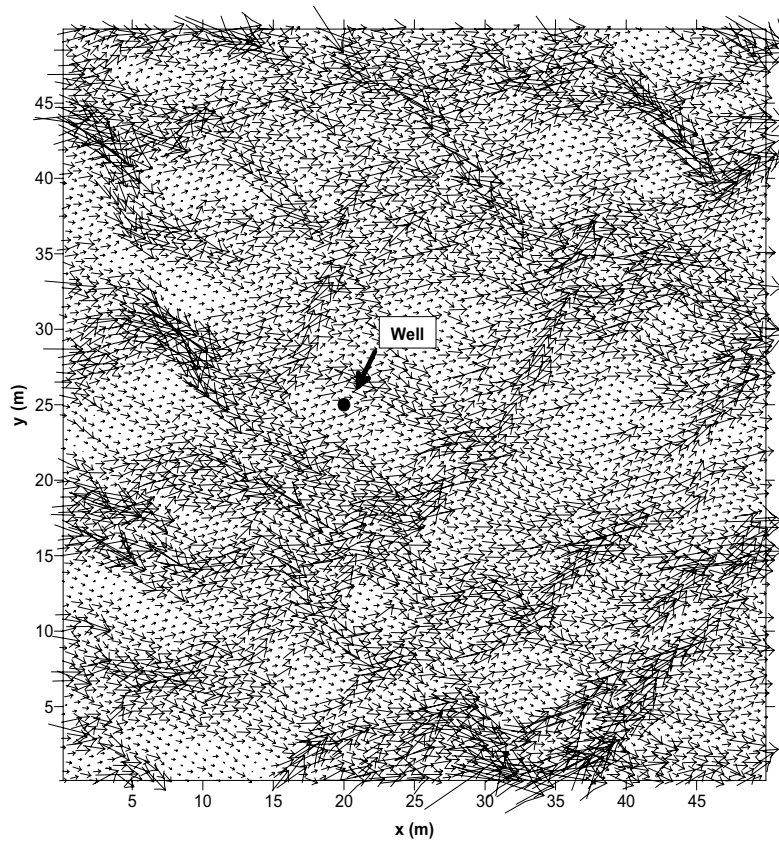


Figure 4-8. Flow vectors without pumping (natural gradient only).

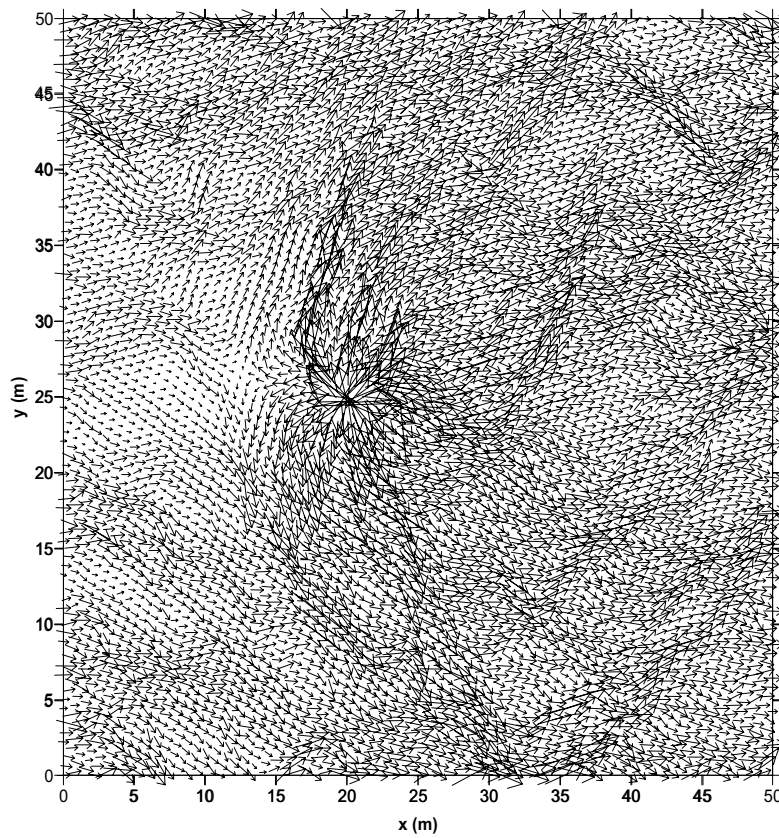


Figure 4-9. Flow vectors during the injection and chaser fluid phases.

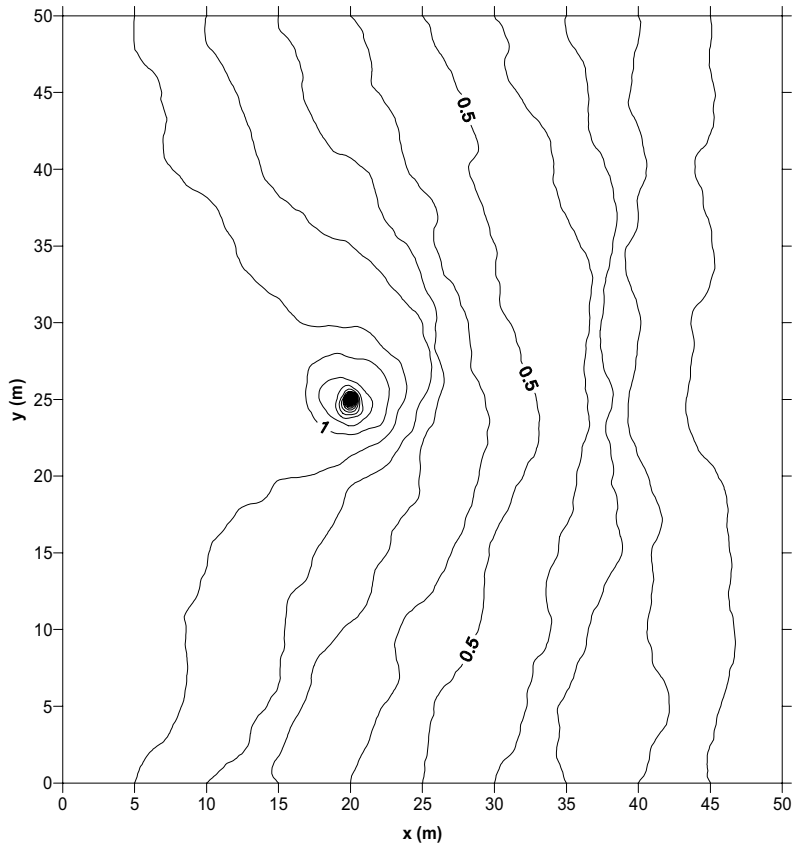


Figure 4-10. Hydraulic head distribution during the injection and chaser fluid phases.

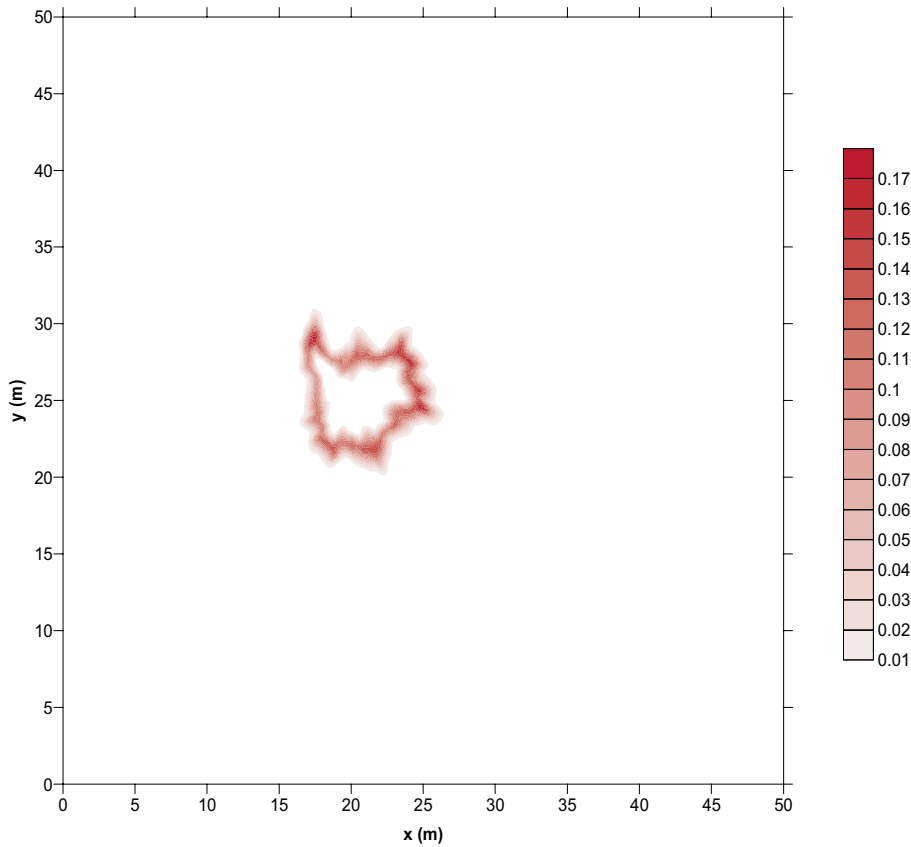


Figure 4-11. Tracer distribution at the end of the chaser fluid phase (i.e. at start of the recovery phase).

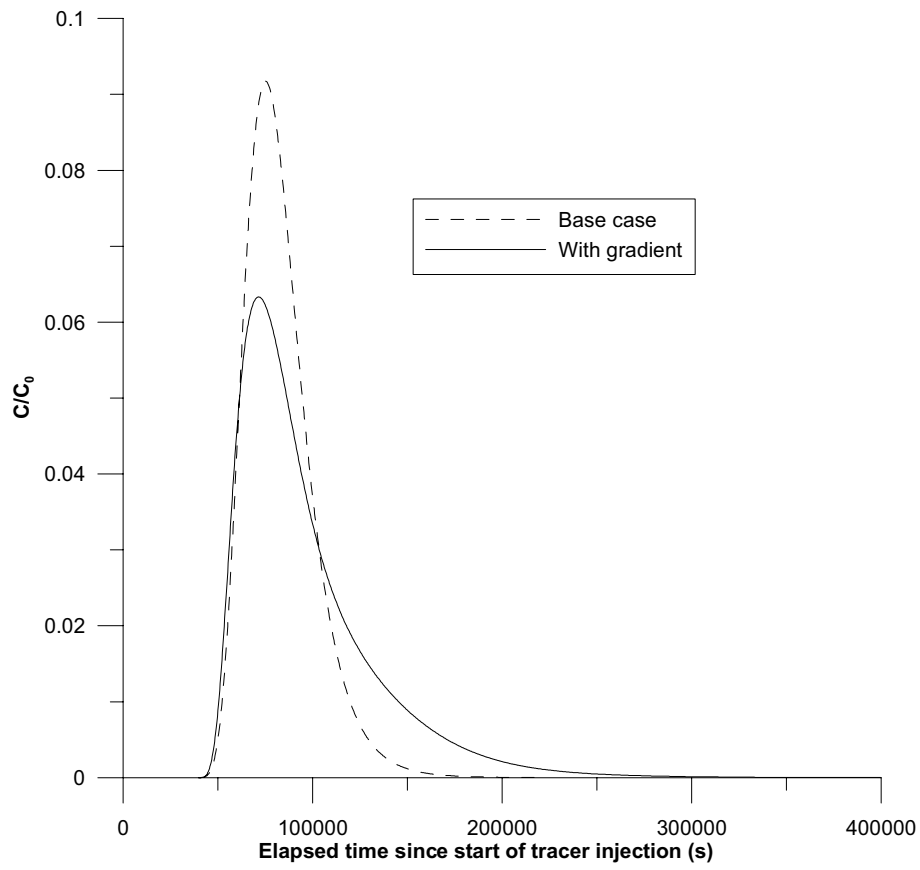


Figure 4-12. Tracer breakthrough curve during the recovery phase for the base case and a background hydraulic gradient.

4.3.1 Evaluation of the base case with hydraulic gradient

Best-fit estimate with gradient assumed known

A regression analysis with p , a_L and pf as estimation parameters were run, with the assumption that the “true” natural background gradient of 0.02 is known independently. The following results were obtained (with standard errors in percent of the estimated value):

$$p = 1.049 \times 10^{-3} (0.981)$$

$$a_L = 0.105 \text{ m} (0.948)$$

$$pf = 0.981 (0.187)$$

The values of linear correlation between the parameters are in this case as follows:

$$p - a_L \quad 0.4736$$

$$p - pf \quad -0.3351$$

$$a_L - pf \quad 0.3439$$

The best-fit regression result is shown in Figure 4-13.

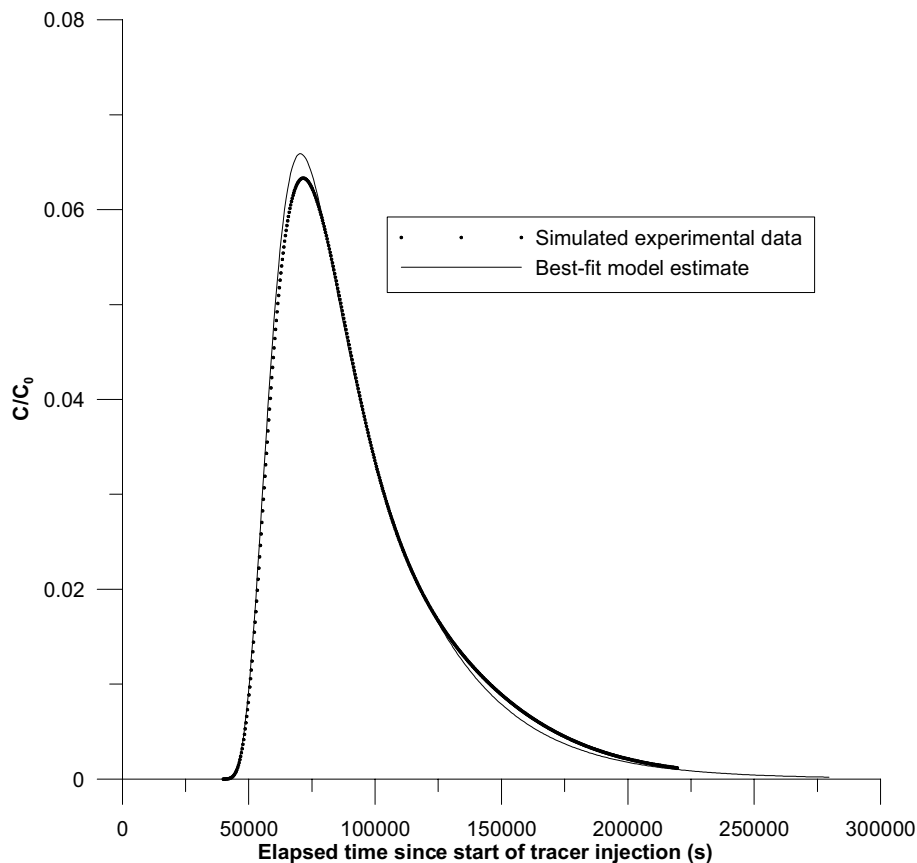


Figure 4-13. Best-fit regression result for the base case with a background natural gradient assumed to have value of 0.02.

The fit is only slightly worse than for the preceding case with no gradient and for an actual field test this would likely be deemed as a relatively satisfactory interpretation. However, this result was obtained with the assumption that the large-scale gradient is known (presumably from groundwater head measurements in other boreholes) and also that the large-scale gradient, together with the transmissivity, provide representative values for the local groundwater flow through the borehole section. In a heterogeneous feature, the local flow may be quite different, and in the example below an alternative interpretation using a “measured” gradient is presented.

Best-fit estimate with “measured” gradient

The preceding evaluation was made with the assumption that the background hydraulic gradient was known independently and the assumed value of the gradient was the actual large-scale gradient used in the model simulation, as defined by the constant-head boundary conditions. In an actual field case, this would correspond to a situation where there were sufficient head measurements in other surrounding boreholes to deduce the magnitude of the overall hydraulic gradient.

However, due to the heterogeneity, the large-scale gradient may not be representative for the local flow through the borehole section where the SWIW test is carried out, or information about the natural gradient may not be present at all. In either case, an appealing approach may be to, prior to the SWIW tests, estimate the natural flow through the section by a dilution test. Combined with an estimate of the transmissivity from a hydraulic test, the hydraulic gradient across the borehole may then in principle be obtained by:

$$\frac{dh}{dl} = \frac{Q_{sec}}{TW} \quad (4-1)$$

where dh/dl [L/L] is the hydraulic gradient in the flow direction l , Q_{sec} [L³/T] is the estimated (from a dilution test) flow rate through the borehole section, T [L²/T] is the transmissivity and W [L] is the effective width of the stream tube for which the flow is determined (often assumed to be twice the borehole diameter).

As a more realistic alternative to the preceding evaluation where the gradient was assumed known and set to the average gradient across the entire model, the gradient was estimated from a simulated dilution test in the tested borehole section. The dilution test was simply simulated by setting the initial condition in the borehole node to 1.0 and then run the model with flow only entering through the boundaries of the model (i.e. no pumping). The result of the dilution test is plotted in Figure 4-14.

In a dilution test, the flow through the tested borehole section is determined from the slope of the straight line resulting from a plot of $\ln C/C_0$ against time as given by the simple mass balance equation for the dilution:

$$\ln \frac{C}{C_0} = \frac{Q_{sec}}{V_{sec}} t \quad (4-2)$$

where C_0 [M/L³] is the initial concentration and V_{sec} [L³] is the volume of the section. With the slope obtained from Figure 4-14 and an effective section volume (V_{sec}) of 4.0×10^{-5} m³ (obtained from the definition of mesh size and porosity in the simulation model) the resulting flow (Q_{sec}) is approximately 6.55×10^{-10} m³/s through the simulation node representing the tested well section. This value is lower than the average flow across the inflow or outflow boundaries, where the average flow per node is about 5×10^{-9} m³/s. This result is consistent with Figure 4-8 which indicates that the tested well in this case is not located in one of the dominating flow paths.

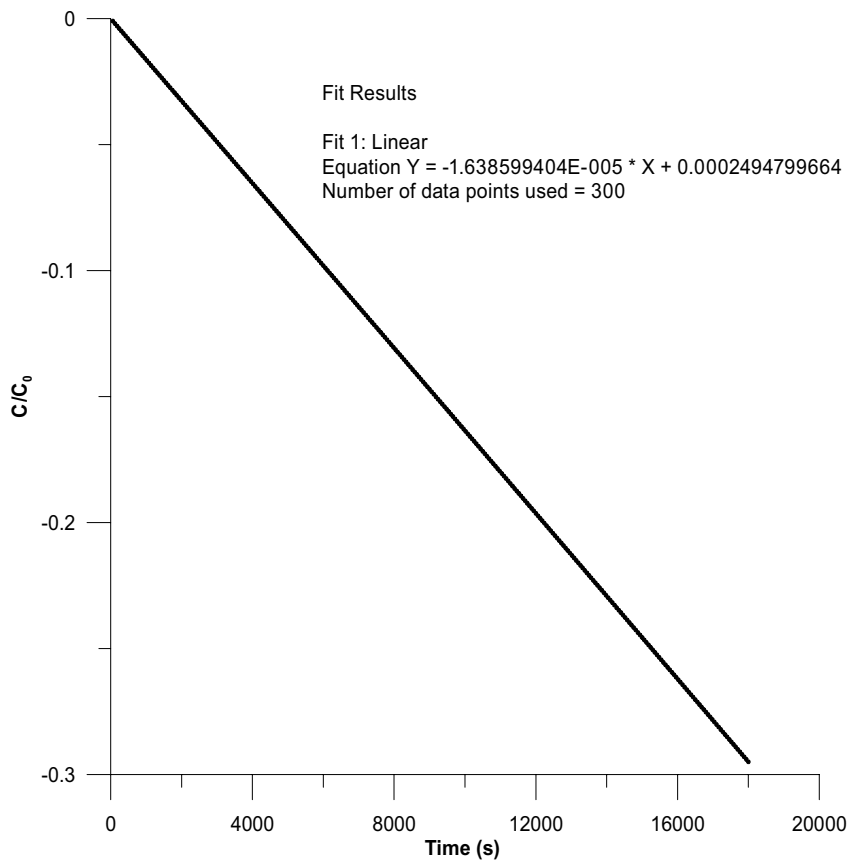


Figure 4-14. Results of a simulated dilution test for the base case with an average hydraulic gradient of 0.02.

The local hydraulic gradient across the tested section is then obtained from eq 4-1. The effective stream tube width is defined by the mesh dimensions and is set to a value of 0.2 m. A simulated hydraulic injection test is used to determine the transmissivity T , which results in a value very close to the assumed average value of 10^{-6} m²/s. This results in a value of approximately 0.0033, which is significantly lower than the large-scale average value of 0.02.

The best-fit estimate when the lower value of the hydraulic gradient (as obtained from the simulated dilution test) results in both different parameter values and poorer estimation statistics. The following results were obtained in this case (standard errors in percent in parenthesis):

$$p = 7.22 \times 10^{-4} (68.1)$$

$$a_L = 0.259 \text{ m} (34.0)$$

$$pf = 0.945 (0.60)$$

At such a low gradient, the correlation between p and a_L is very high, which causes the large standard errors of these parameters.

4.3.2 Tracer injection in a major flow path

In the preceding example, the injection well happened to be located in a relatively low-flowing area (see Figure 4-8). As an alternative, an identical simulation scenario was run where the well was placed in one of the apparently dominating flow paths. The location of the well in this case is shown in Figure 4-15 below.

The resulting tracer plume at the end of the chaser injection phase is shown in Figure 4-16, and shows that one part of the plume extends in the flow direction of the dominating flow path.

The tracer recovery curve for this case is shown in Figure 4-17, together with the corresponding curves for the base case well location with and without hydraulic gradient, respectively. The appearance of the tracer recovery curve for the case of injection in a high flow area differs from, and look more irregular than, the case with injection in a low flow area (base case).

A simulation of a dilution test, as was done above for the base case well location, indicates a flow through the well node of about $5 \times 10^{-9} \text{ m}^3/\text{s}$, which would imply a gradient of about 0.025.

A regression was carried out with three estimation parameters: p , a_L and pf . The best-fit parameters were as follows (with standard errors in percent):

$$p \quad 6.55 \times 10^{-4} \text{ (3.2)}$$

$$a_L \quad 0.208 \text{ m (3.5)}$$

$$pf \quad 1.01 \text{ (0.89)}$$

The best-fit tracer recovery curve is shown in Figure 4-18. As expected, it is in this case not possible to fit the irregularity of the simulated tracer recovery curve, which is due to the flow heterogeneity around the well.

The standard errors of the estimated values are low and all values of correlation between parameters are moderate in this case.

It may be mentioned here that a SWIW test simulation (not shown) in the same location, but with no overall natural gradient, resulted in very similar results as for the base case well location.

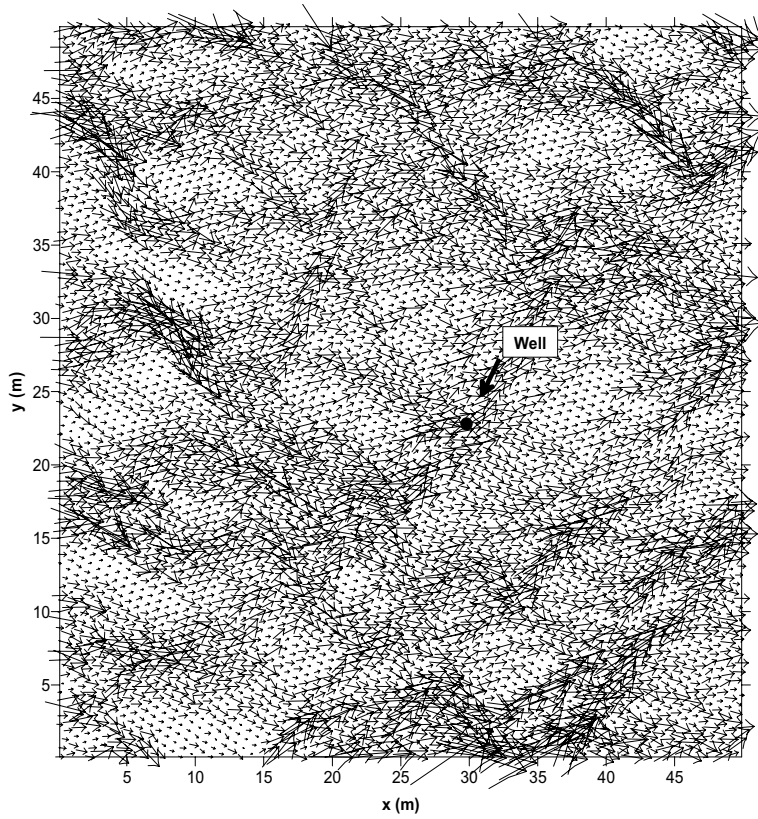


Figure 4-15. Location of well with flow vectors showing the natural flow field. The well is in this case placed in a relatively major flow path.

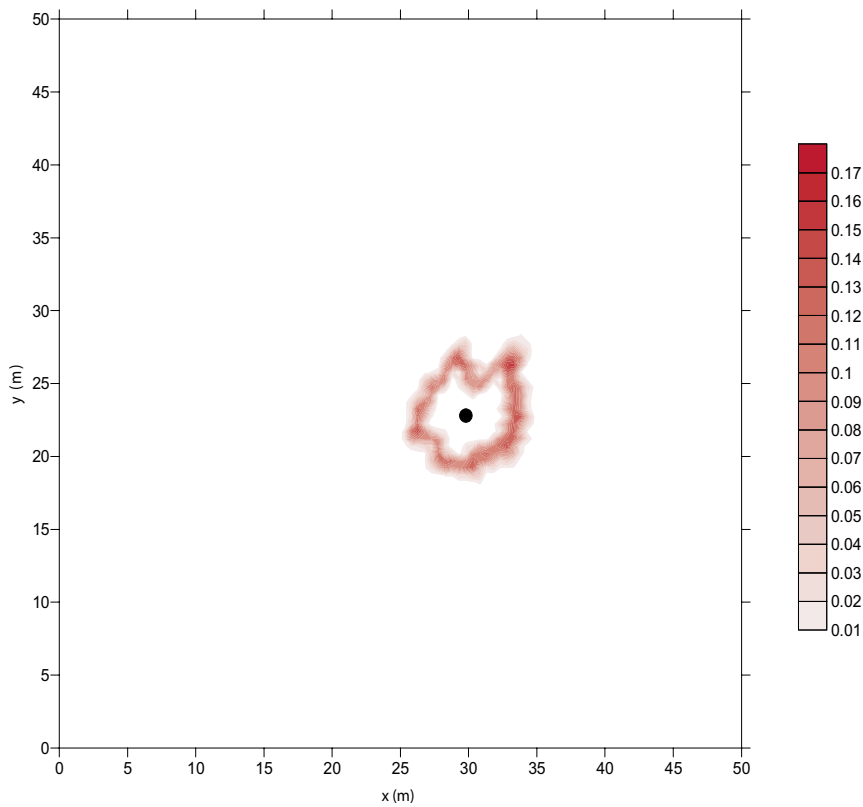


Figure 4-16. Tracer concentration distribution at the end of the chaser injection period.

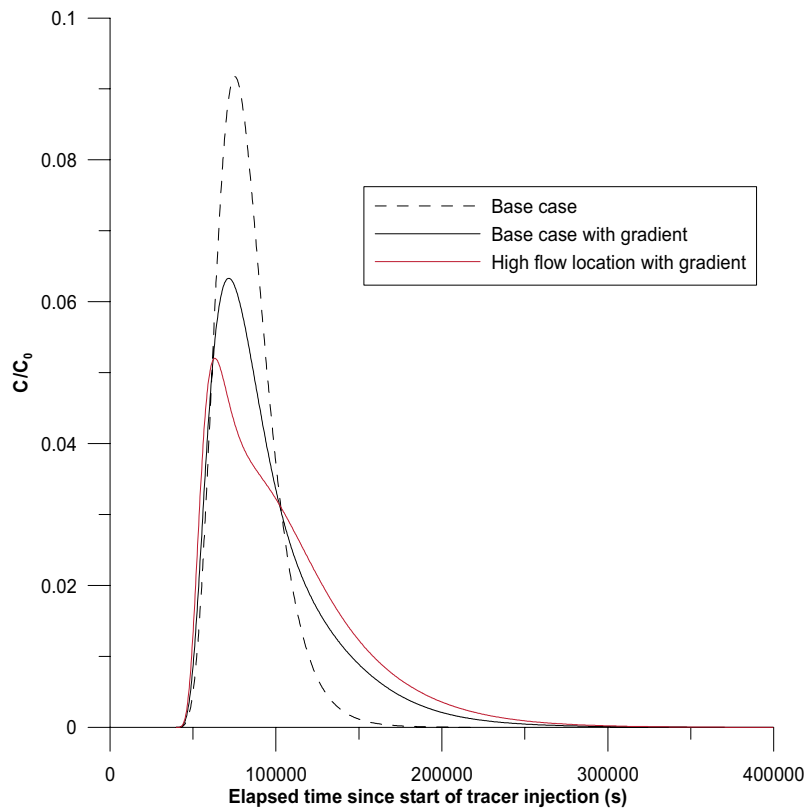


Figure 4-17. Tracer recovery for the case of a well located in a high flow area compared with the base case location.

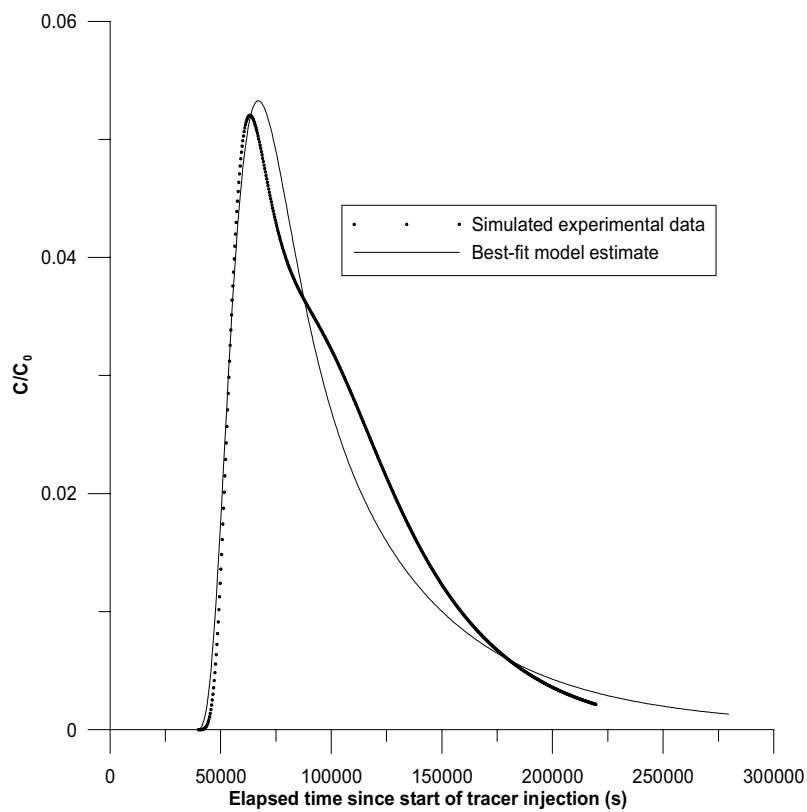


Figure 4-18. Best-fit estimate of tracer recovery data for the high flow base case location.

4.4 Case 2 simulations

In the second main case, a simulated feature with increased heterogeneity, compared with the base case, was used. The variance of $\ln(T)$ was set to 5 and the correlation length to 5 m. The generated $\ln(T)$ field is shown in Figure 4-19.

The tracer recovery for a simulated SWIW test, performed at the same location as for the base case above, is shown in Figure 4-20 together with a best-fit estimate with a homogenous model. The recovery curve and the regression results for this case are very similar to the corresponding results obtained for the base case.

As was done for the base case, simulated SWIW tests with a natural hydraulic gradient with a magnitude of 0.02 were run for two different well locations. The locations are shown in Figure 4-21, where the flow field also is illustrated. The natural flow rates through the well sections, as determined from simulated dilution tests, are $2.05 \times 10^{-10} \text{ m}^3/\text{s}$ and $3.57 \times 10^{-9} \text{ m}^3/\text{s}$ for the low-flow and high-flow locations, respectively.

The resulting tracer recovery curve for the SWIW tests in the two wells are shown in Figure 4-22. Similar to the corresponding result for the base case, the tracer recovery curve for the high-flow location has somewhat more irregular features.

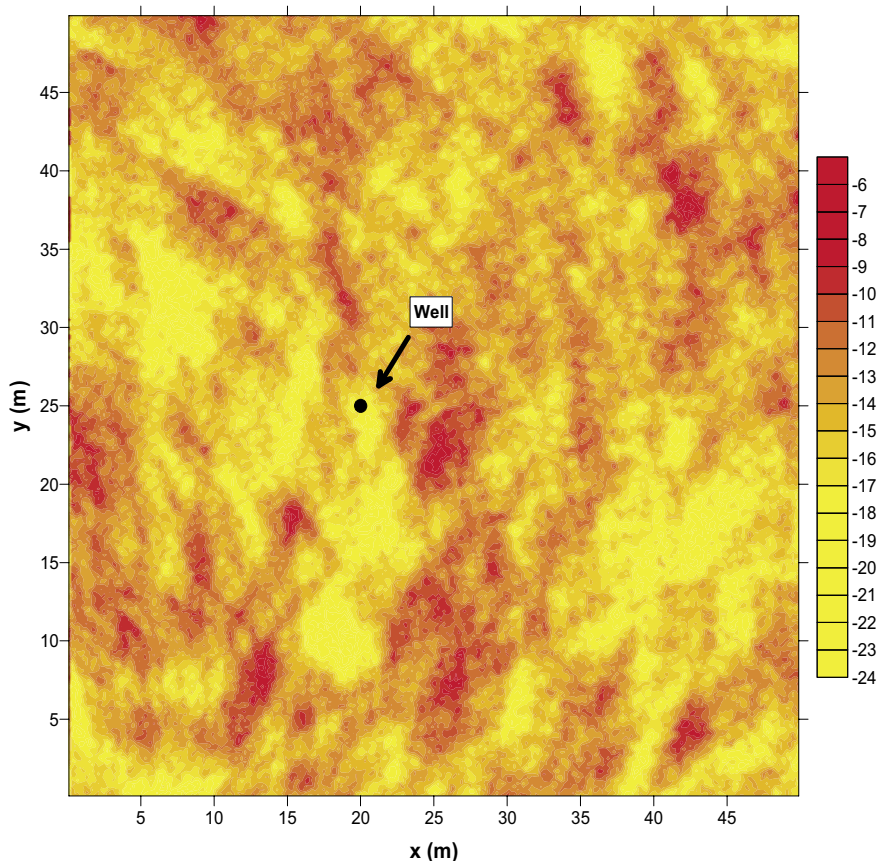


Figure 4-19. Spatial distribution of $\ln T$ for case 2 simulations.

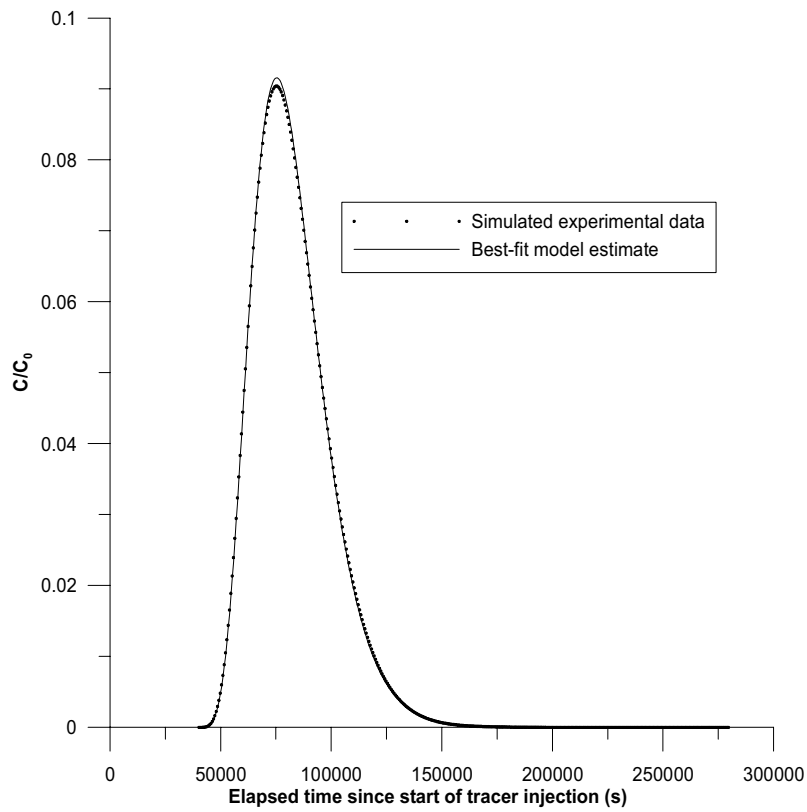


Figure 4-20. Simulated tracer recovery curve and best-fit regression estimate for case 2 without hydraulic gradient.

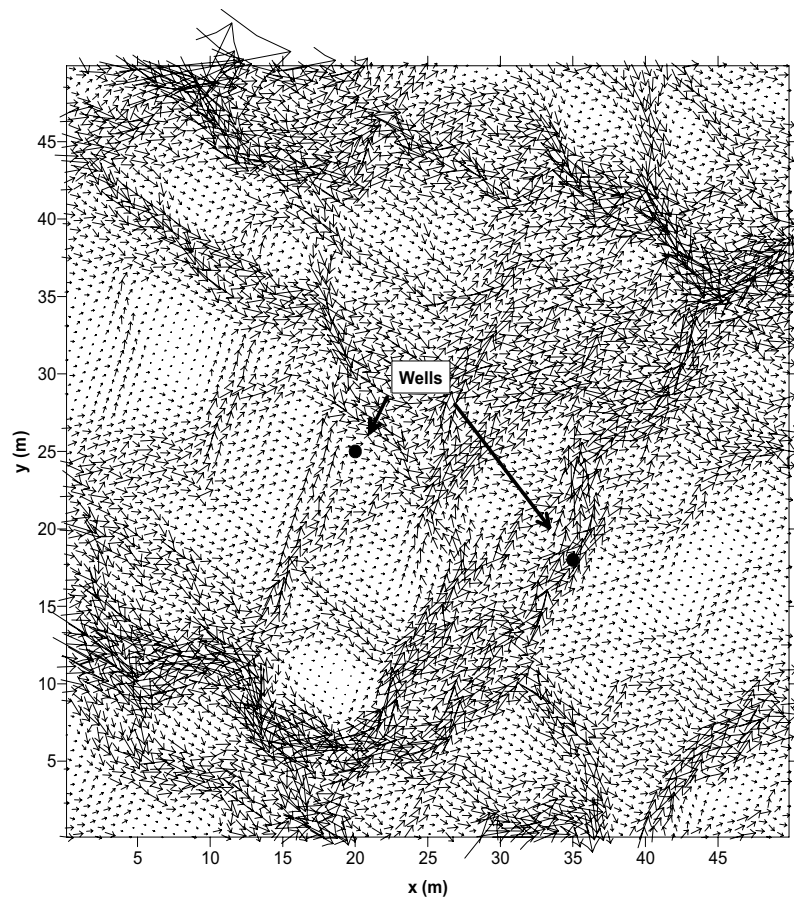


Figure 4-21. Flow vectors and test locations for case 2 SWIW tests with a natural gradient.

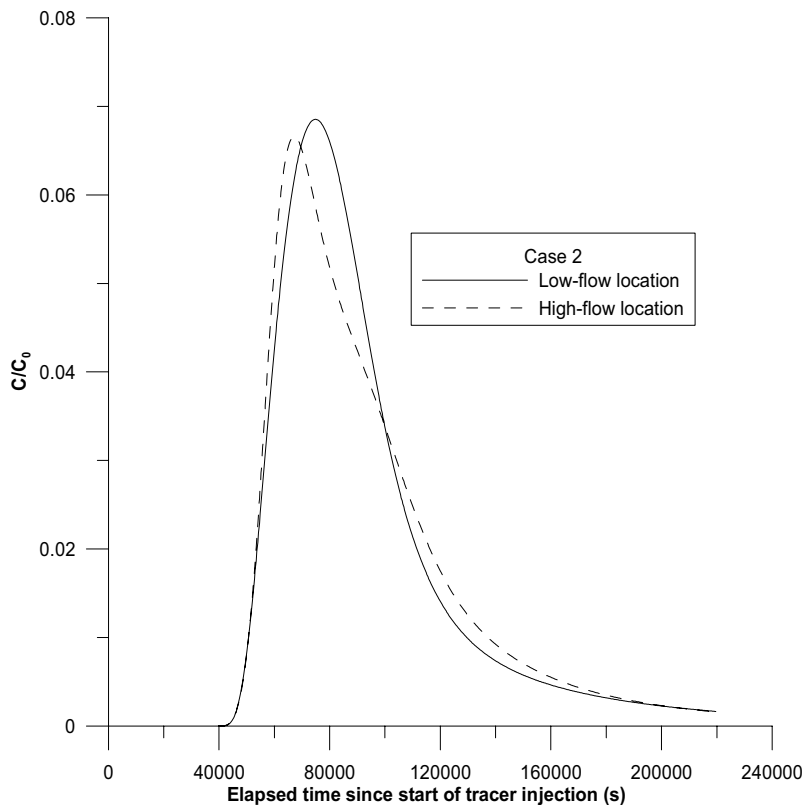


Figure 4-22. Tracer recovery curves for case 2 SWIW test simulations with a hydraulic gradient of 0.02.

4.5 Simulations with sorbing tracers

4.5.1 Base case simulations

A simulation with a tracer undergoing linear equilibrium sorption was run for the base case, setting the retardation factor, R , equal to two. In a cross-hole tracer test, this would mean that the residence time for the sorbing tracer should be twice that of a conservative tracer and the visible difference in breakthrough curves would be relatively large. In a SWIW test, on the other hand, differences in the tracer recovery curves are expected to be much less visible. In fact, in absence of hydrodynamic dispersion, there would be no difference at all in the arrival of tracers with different retardation factors during the tracer recovery phase.

The tracer recovery breakthrough curve for the base case is shown in Figure 4-23. The resulting curve for the sorbing tracer is fairly typical for linear equilibrium sorption and is very similar to earlier results for homogeneous conditions /Nordqvist and Gustafsson, 2002/.

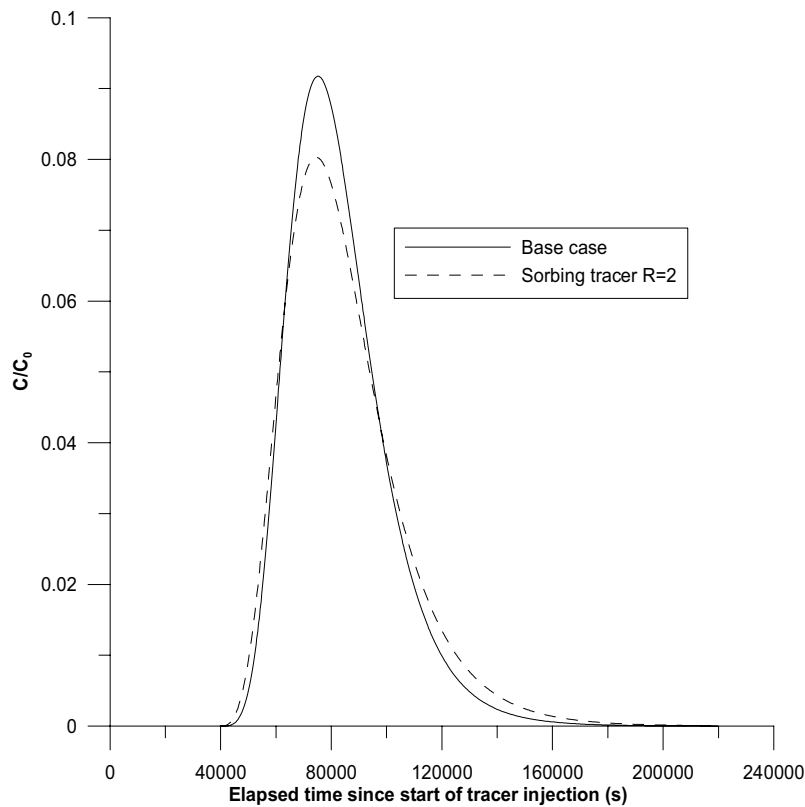


Figure 4-23. Tracer recovery of a tracer with $R=2$ compared with a non-sorbing tracer.

A regression analysis was carried out with an estimation scenario of a_L , pf and R (the retardation factor) as estimated parameters. Regression analysis involving sorbing tracers were carried out in the manner described in section 3.5, with simultaneous analysis of non-sorbing and sorbing tracer recovery curves. This resulted in the following best-fit parameters (with standard errors in percent):

$$a_L \quad 0.097 \text{ (0.19)}$$

$$pf \quad 0.999 \text{ (0.055)}$$

$$R \quad 1.86 \text{ (0.993)}$$

and the following values of correlation between parameters:

$$a_L - pf \quad 0.479$$

$$a_L - R \quad -0.616$$

$$pf - R \quad -0.017$$

The best-fit tracer recovery curves are shown in Figure 4-24.

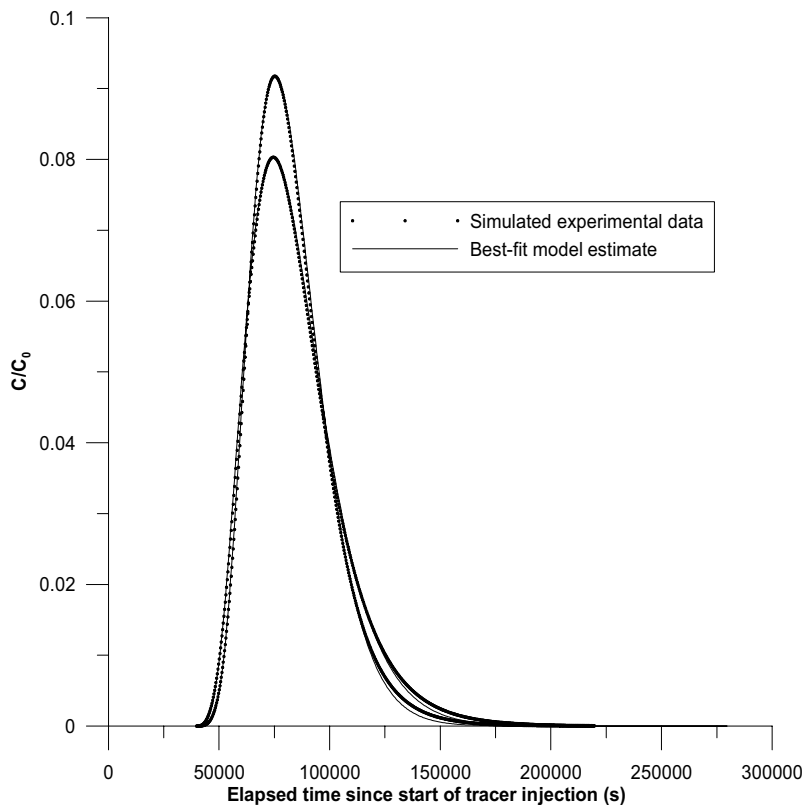


Figure 4-24. Best-fit tracer recovery curve for the base case with a non-sorbing and a sorbing tracer injected simultaneously (the sorbing tracer has the lower maximum value).

4.5.2 Sorbing tracers with a hydraulic gradient

In this case, a natural gradient of 0.02 was added to the preceding case. The resulting breakthrough curve is shown in Figure 4-25. In contrast to the case without hydraulic gradient, the recovery curve for the sorbing tracer appears to be less dispersed and with a higher peak concentration than the non-sorbing tracer. This is apparently an effect of the presence of the background gradient which has a larger effect on the non-sorbing tracer than the sorbing tracer. Results from simulations with homogenous conditions (not shown here) indicate that this effect does not seem to occur in such environments. However, it has not been thoroughly examined whether some combinations of gradient magnitude and retardation factors may cause interpretation ambiguity regarding sorption also in homogenous formations.

The same general effect can be seen in other simulation examples. The recovery curve of a sorbing tracer, for the previously analysed case with a high-flow well location in the base case feature, is shown in Figure 4-26 and the result for case 2 with a gradient and a sorbing tracer is shown in Figure 4-27.

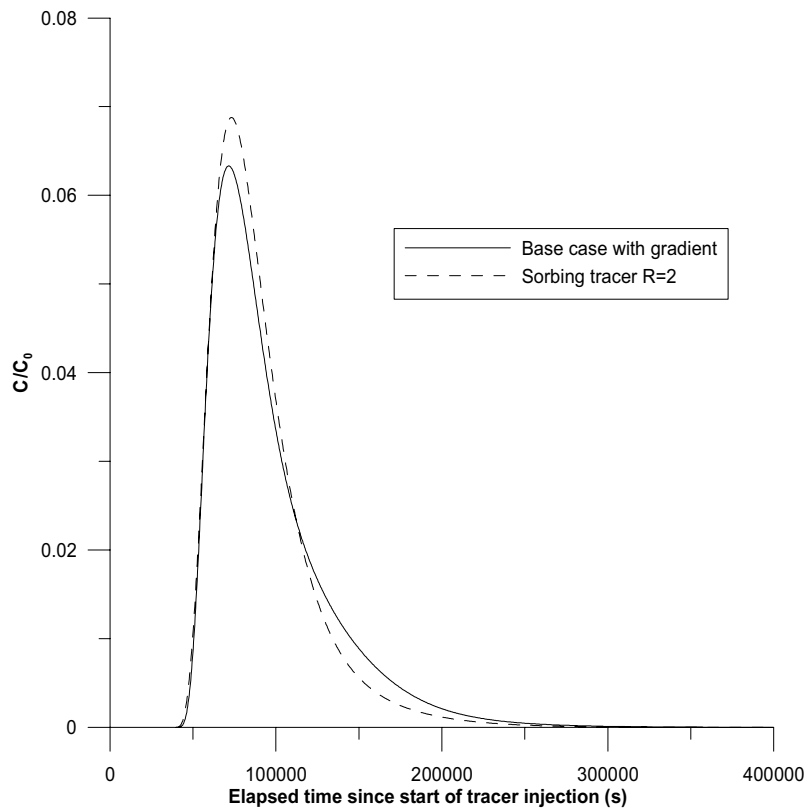


Figure 4-25. Comparison of sorbing and non-sorbing tracer recovery curves for the base case with a hydraulic background gradient of 0.02.

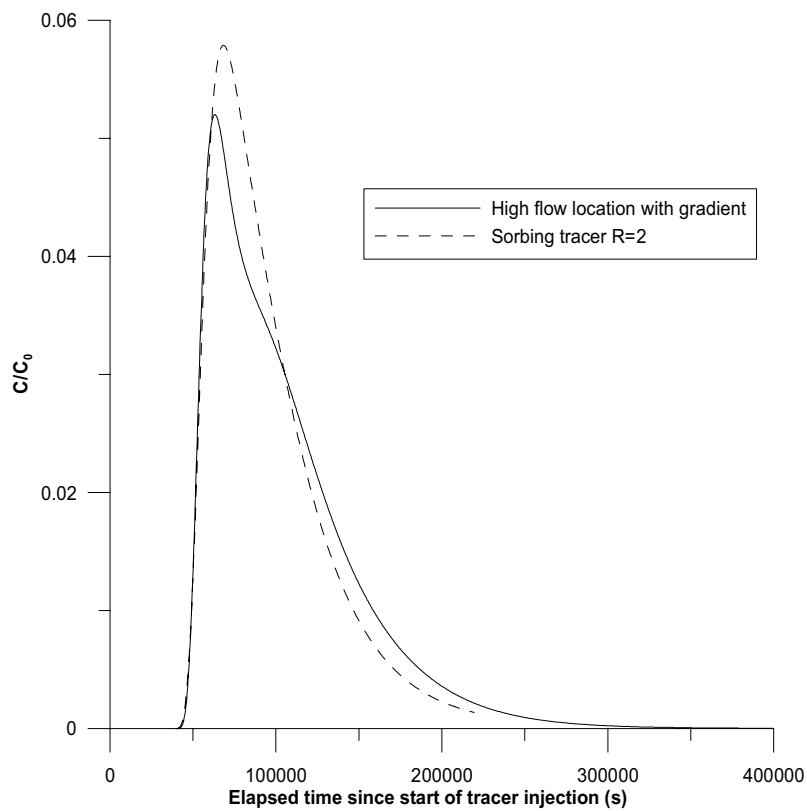


Figure 4-26. Tracer recovery curves for a non-sorbing and sorbing tracer, respectively, in the base case heterogeneous feature and the well located in a high-flow area (see Figure 4-15).

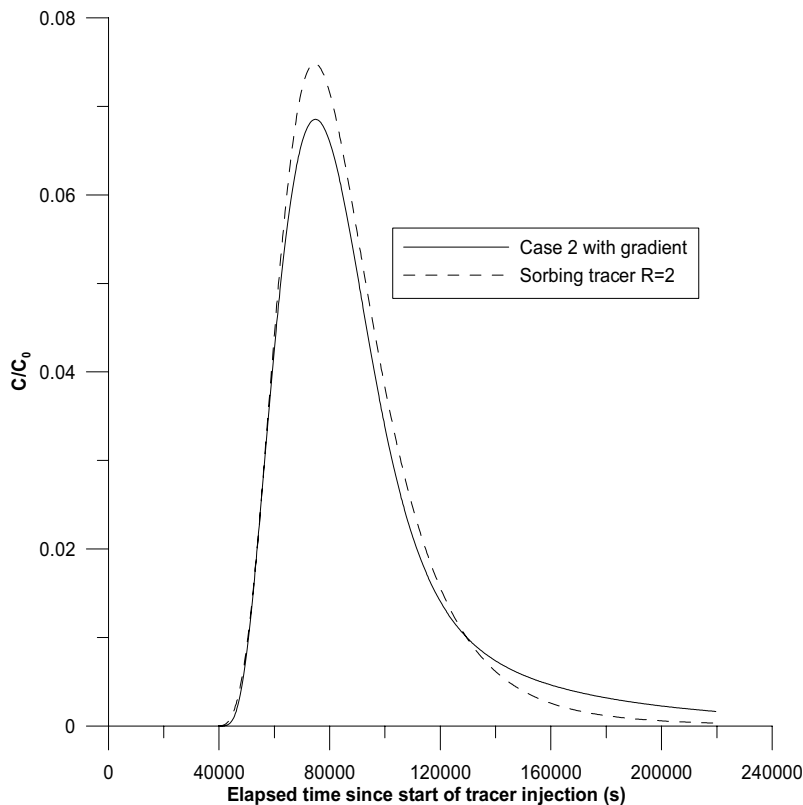


Figure 4-27. Tracer recovery curve for a non-sorbing and sorbing tracer, respectively, in the case 2 heterogeneous feature with a natural hydraulic gradient.

In the shown cases with sorbing tracers and a significant natural flow through the tested borehole section, the breakthrough curves for sorbing and non-sorbing tracers, respectively, are apparently “reversed” compared to what would be expected for homogeneous conditions. Whether this effect would be generally expected to occur in heterogeneous features with a background flow may probably not be concluded based the few simulations shown here, and reports of such effects have not been found in the existing literature.

Regression analysis would in all of the shown cases assuming a background gradient, using the homogeneous estimation model, not result in any reliable estimates of retardation factors or other parameters. The few cases examined suggest that interpretation of sorption may generally be difficult in the presence of significant background flows through the tested borehole section in combination with heterogeneity around the section.

4.5.3 Implications for interpretation of matrix diffusion effects

Based on the results from the various preceding simulation cases, it is also possible to indicate some implications for interpretation of matrix diffusion effects from SWIW test results in heterogeneous environments. Of primary importance is whether there is a significant natural (or induced by tunnels, etc) flow through the tested section.

In the case of no or very low background flow rates (i.e. low gradients), heterogeneity does not cause anomalous effects. Irrespective of to what extent transport is channelised (i.e. affected by heterogeneity), flow reversibility would be expected to occur. Thus, differences between breakthrough curves from tracers with different diffusion properties would be visible and relatively intuitive in appearance.

In the presence of significant background flow, flow reversibility may not always occur in a SWIW test. The simulations with sorbing tracers indicate that it is possible that such effects may not be unlikely. The interpretation difficulties that are indicated in this report for sorbing tracers may be expected to be at least as aggravating for interpretation of matrix diffusion effects under conditions of high natural flow rates and heterogeneity. During tests for studying matrix diffusion, a waiting phase may also be included and adverse effects of natural flow rates may then be even larger.

The implications listed above for interpreting matrix diffusion are consistent with results from a study by /Lessoff and Konikow, 1997/. In this study, it was found that background hydraulic gradients in combination with heterogeneity may lead to advective effects that would give similar effects as matrix diffusion on the tracer breakthrough curves. This effect would be aggravated by employing a long waiting phase.

The identification and possible quantification of processes such as sorption and matrix diffusion, from SWIW tests and other tracer experiments, relies on that tracers with different properties are injected simultaneously and that the differences may be used to deduce effects of processes. The simulations in this report indicate that such interpretation may be difficult for either sorption or diffusion under conditions of high background flows and heterogeneity. This further emphasizes the importance of prior information about hydraulic conditions (i.e. transmissivity and background flow) in the tested borehole section.

5 Summary and conclusions

- This study presents a few examples of SWIW tests in heterogeneous formations. Heterogeneity is limited to variations in the transmissivity (variance and correlation length), which has the effect of creating paths of preferential flow for the flowing groundwater. Heterogeneity in other attributes, such as porosity or sorption properties, is beyond the scope of this study.
- An example of an evaluation methodology involving automatic parameter estimation based on homogeneous assumptions has been demonstrated, analogous to typical simple one-dimensional models used for basic evaluation of tracer breakthrough curves from cross-hole tests. It is not unlikely that such an approach will be one of the basic tools used for the interpretation of actual field tests. It is envisioned that one of the best uses of SWIW tests is simultaneous injection of more than one tracer with, for example, different sorption and/or diffusion properties. The evaluation methodology presented here provides an example of how recovery breakthrough curves of several tracers may be interpreted simultaneously. One important aspect of the evaluation methodology is the simultaneous interpretation of multiple tracer recovery curves.
- Despite heterogeneous flow conditions, the simulated SWIW tests often produce apparently “well-behaved” (i.e. similar to results for homogeneous conditions) tracer recovery curves because the injected water returns along the same flow paths, thereby obscuring the effects of heterogeneity on the flow pattern.
- In the examples studied, parameter estimation using a homogeneous approach works relatively well in environments with a low background flow, regardless of the location of the well. Estimated parameter values differ only moderately between different estimation scenarios.
- Prior knowledge of some parameters may be important for the interpretation of SWIW tests, such as information about porosity/aperture. In the presence of a natural hydraulic gradient, estimation of the gradient across the tested borehole during the SWIW test may be a potential problem.
- The presence of a significant background hydraulic gradient appears to potentially result in irregular breakthrough curves, at least for cases when the tested well is located in a major flow path. It is possible that a systematic study might show that this happens only if the well is located in a major flow path and, if so, this in itself may be an interpretation possibility of SWIW tests.
- In the examples studied, the presence of a significant hydraulic gradient, combined with heterogeneity, appears to cause interpretation problems for sorbing tracers. This may indicate that sorbing tracers are best studied in borehole sections with very low natural flow rates. Generally, it is possible that the specific purpose of each individual SWIW test may depend on the prevailing hydraulic conditions.

- Matrix diffusion processes were not simulated explicitly in this study. However, the results herein regarding sorbing tracers, together with findings from other studies, generally support arguments that diffusion experiments are best suitable for low flow environments, because of possible effects of flow irreversibility.
- Although studies using synthetic features with heterogeneous transmissivity may help to illustrate potential interpretation problems caused by heterogeneity, a necessary next step should be to perform and analyse results from actual SWIW field tests. This will provide experimental reference data that likely also will introduce additional aspects from an interpretation point-of-view. In order to further investigate interpretation aspects, field tests should preferably also be complemented by hydraulic tests and tracer dilution tests.

6 References

- Altman S J, Jones T L and Meigs L C, 2000.** Controls on mass recovery for single-well injection-withdrawal tracer tests. Chapter 4 in Sandia report SAND97-3109 (Meigs et al, editors).
- Andersson P, 1995.** Compilation of tracer test in fractured rock. SKB Progress Report 25-95-05. Svensk Kärnbränslehantering AB.
- Andersson P, Byegård J and Winberg A, 2002.** Final report of the TRUE Block Scale project. 2. Tracer tests in the block scale. SKB Technical Report TR-02-14. Svensk Kärnbränslehantering AB.
- Andersson P, Byegård J, Tullborg E-L, Doe T, Hermansson J, Winberg A, 2003.** Studies of block scale tracer retention properties in crystalline rock, Äspö HRL, Sweden. Results of in situ sorbing tracer experiments and a first attempt of 1D modelling. Journal of Contaminant Hydrology (in press).
- Cooley R L, 1979.** A method of estimating parameters and assessing reliability for models of steady state ground water flow. 2. Application of statistical analysis. Water Resources Research 15: 603–617.
- Lessoff S C and Konikow L K, 1997.** Ambiguity in measuring matrix diffusion with single-well injection/recovery tracer tests. Ground Water 35, no 1: 166–176.
- Levenberg K, 1944.** A method for the solution of certain nonlinear problems in least squares. Q. Appl. Math., 2: 164–168.
- Mantoglou A and Wilson J L, 1989.** Simulation of random fields with the Turning Bands Method, Rep. 264, Dept. of Civ. Eng., Mass. Inst. of Technol., Cambridge.
- Marquardt D W, 1963.** An algorithm for least squares estimation of non-linear parameters. J. Soc. Ind. Appl. Math. 11: 431–441.
- Nordqvist R, 1998.** Scoping calculations for tests with sorbing tracers at the TRUE-1 site: The impact of different experimental strategies on parameter estimation. HRL-98-05, 33p. Svensk Kärnbränslehantering AB.
- Nordqvist R and Gustafsson E, 2002.** Single-well injection-withdrawal tests (SWIW). Literature review and scoping calculations for homogeneous crystalline bedrock conditions. SKB R-02-34. Svensk Kärnbränslehantering AB.
- Tsang Y W, 1995.** Study of alternative tracer tests in characterizing transport in fractured rocks. Geophysical Research Letters 22, no 11: 1421–1424.
- Van Genuchten M Th and Alves W J, 1982.** Analytical solutions of the one-dimensional convective-dispersive solute transport equations. Tech. Bull. 1661, 151p. U.S. Dept. Of Agriculture, Washington D.C., 149p.
- Voss C I, 1984.** SUTRA – Saturated-Unsaturated Transport. A finite element simulation model for saturated-unsaturated fluid-density-dependent ground-water flow with energy transport or chemically-reactive single-species solute transport. U.S. Geological Survey Water-Resources Investigations Report 84-4369.